



UNIVERSITÀ DI PARMA

ARCHIVIO DELLA RICERCA

University of Parma Research Repository

Morphological changes of the floodplain reach of the Taro River (Northern Italy) in the last two centuries

This is a pre print version of the following article:

Original

Morphological changes of the floodplain reach of the Taro River (Northern Italy) in the last two centuries / Clerici, Aldo; Perego, Susanna; Chelli, Alessandro; Tellini, Claudio. - In: JOURNAL OF HYDROLOGY. - ISSN 0022-1694. - 527:(2015), pp. 1106-1122. [10.1016/j.jhydrol.2015.05.063]

Availability:

This version is available at: 11381/2789931 since: 2021-10-11T11:46:52Z

Publisher:

Elsevier

Published

DOI:10.1016/j.jhydrol.2015.05.063

Terms of use:

Anyone can freely access the full text of works made available as "Open Access". Works made available

Publisher copyright

note finali coverpage

(Article begins on next page)

05 July 2024

A. Clerici, S. Perego, A. Chelli, C. Tellini

Department of Physics and Earth Sciences, University of Parma, Italy

Morphological changes of the floodplain reach of Taro River (Northern Italy) in the last two centuries

Abstract

The quantitative analysis of the planform changes of the unconfined reach of the Taro River, in the Italian Northern Apennines, has been carried out in order to outline the channel evolution in the last 200 years.

Nine sets of maps and orthophotos, ranging from 1828 to 2011, have been used to evaluate the medium-term changes in channel morphology in the entire time interval and the short-term changes in the most recent decade. Starting from the digitized channel limits and bars, a number of shell scripts based on the GRASS GIS commands have been used for a fast and automatic calculation of the main morphological parameters (channel length, width, braiding, sinuosity, centerline shifting) and the drawing of graphics showing in detail their continuous variations along the entire study reach. The analysis of the parameters differences of subsequent dates revealed, at least until the end of the 20th century, a continuous reduction of channel width (up to a total of 75%) and braiding (43%), and a continuous increase of channel length (13%) and sinuosity (29%), in agreement with most of the previous studies on other rivers both in Italy and abroad. In contrast with the results of other studies, the most recent evolutionary trend of Taro R. shows a substantial morphological stability in the upper multi-thread part of the channel and a slight persistent narrowing in the lower single-thread. The analysis of the variations along the channel, facilitated by the curves of the parameters and supported by the historical documentation, reveals that these variations can be substantially attributed to the human activity. In particular, the continuous narrowing is largely due to the recurrent subtraction of river areas to be assigned to agriculture and industry, and to the

construction of 10 bridges and their related bank protections. The intense mining between 1950s and 1980s, seems to have provoked a sharp incision and only partially a narrowing. The morphological changes due to the reduction in the flow regime that seems appear from the sporadic and discontinuous hydrological data, should be negligible and in any case relegate in the background by the remarkable changes due to the human activity.

Keywords

Taro River

Northern Italian Apennines

Channel morphological changes

GIS GRASS

Error estimation

1. Introduction

The study of the past morphological changes of floodplain unconfined reaches and the relationship with the natural and human induced controlling factors is widely recognized as a useful instrument to define the evolutionary trend in order to plan a correct river management or a sustainable river restoration. The morphological evolution involves bed level fluctuations, as a consequence of incision and aggrading, and planform changes, concerning channel width, position and pattern. The older channel altimetric variations are impossible to assess for the lack of in-channel elevation values in the old historical maps. In-channel elevation data are anyway limited also for recent periods as they need accurate measurements directly on the field. The planform channel changes on the contrary can be more easily defined in quantitative terms both in the older cartography than in the modern ortophotos through indexes and parameters proposed and experimented since a long time by various authors (channel width, braiding, sinuosity, shifting) and whose acquisition and analysis have been considerably improved by the use of Geographical Information Systems (GIS). Much more difficult is to define the causes of the river modifications. Even though there is a general agree in recognize the river adjustment controlling factors, i.e. climatic changes and antropic activity at catchment and channel scales, the influence of each single factor is difficult to assess especially when the factors act together. The unceasing research of the causes-effects assessment in different world regions is testified by the great number of works dealing with the subject. An updated and exhaustive list of works can be found, for instance, in the recent papers of Ziliani and Surian (2012) and of Segura-Beltrán and Sanchis-Ibor (2013). As regards specifically Italy, many studies on rivers both from Alps and Apennines have been carried out as resumed in Gurnell et al. (2009) and in Comiti et al. (2011).

In the present paper an analysis of the planimetric changes of the floodplain unconfined reach of the Taro River, one of the greater tributary of the Po River in the Northern Italian Apennines, is presented. The analysis has been performed by comparing a sequence of maps and ortophotos ranging from 1828 to 2011. Six of them (1828, 1881, 1958, 1976, 1999, 2011) have been used to

evaluate medium-term changes in channel morphology, while 2003, 2006, 2008 have been used to evaluate the short-term variations of the parameters in the time interval 1999-2011. As the morphometric parameter calculations require a long and repetitive sequence of operations, even if carried out in a GIS environment, a set of shell (or programs) scripts, mainly based on the GIS commands, have been created. These automatically compute the parameters and construct graphics showing the parameters changes along the entire development of the channel, speeding up the procedure and enabling at the same time a detailed analysis of the planform changes in time and space.

In the attempt to explain the measured morphological changes, the available information on hydrological characteristics at gauging stations (rainfall, river discharge and stage) have been collected together with the scanty official data on the amount of in-channel gravel mining. The description of past events contained in the historical archives or reported in more recent books proved to be very useful for the reconstruction of past river conditions.

2. The study reach

The Taro R., located in the Italian Northern Apennines in the Parma Province, flows from the main Apennines divide to the Po R. for about 126 km. The first 72 km, until the Fornovo town, drain a mountainous region, where alloctonous geological formations Tertiary in age prevail. The remaining 54 km are located in the Po plain, formed by successions of marine and continental deposits Plio-Quaternary in age. Of the total drained area of about 2026 km², 800 km² are in floodplain sector (Fig.1).

In Fornovo the Taro R. receives the Ceno Torrent, the most important of its tributaries, that drains a basin of about 526 km². Close to its confluence in the Po R. receives the Stirone Torrent that drains an area of about 300 km².

The river characteristics and evolution appears strongly conditioned by the structural setting of the area. In fact the course of Taro R. coincides with a great fault which activity during the Plio-

Quaternary caused the uplifting of the western side of some tenths of meters (Bernini and Papani, 1987). The main effect is the progressive shift of the channel eastward, as testified by the presence (in the middle and low plain) of paleochannel tracks almost exclusively on the western side of the present channel.

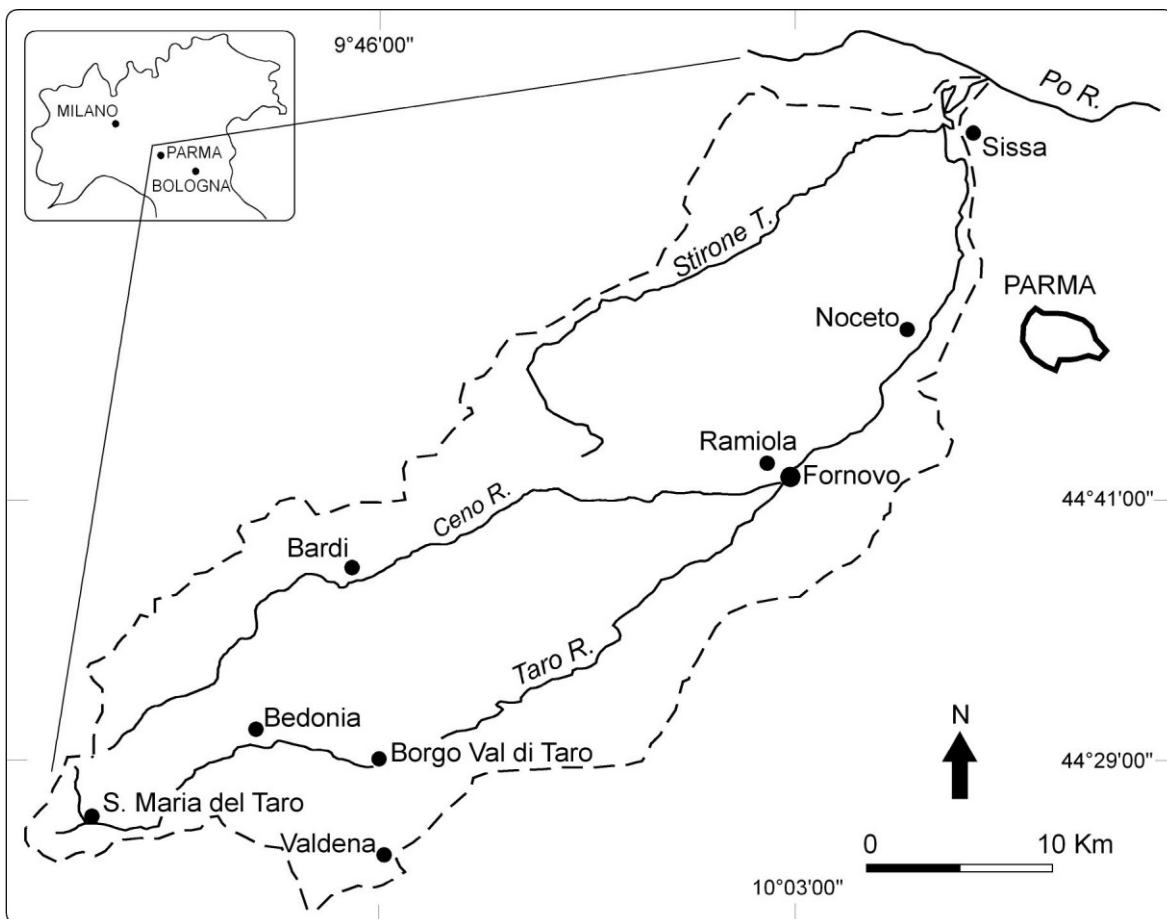


Fig.1. Taro R. basin with the study reach from Fornovo to Po R..

The river characteristics and evolution appears strongly conditioned by the structural setting of the area. In fact the course of Taro R. coincides with a great fault which activity during the Plio-Quaternary caused the uplifting of the western side of some tenths of meters (Bernini e Papani, 1987). The main effect is the progressive shift of the channel eastward, as testified by the presence (in the middle and low plain) of paleochannel tracks almost exclusively on the western side of the present channel.

As regards the channel pattern, presently the unconfined study reach is typically braided in the upper part for about 19 km and typically single-thread and mainly meandering in the lower part for about 29 km. The middle (intermediate) tract of about 6 km is transitional with wandering characters.

Along the basin divide the mean annual precipitation is about 2600 mm (max November 296 mm, min July 68 mm), and the mean annual temperature is 12.0°C (max July 18.6°, min January 1.0°). Close to the mouth the mean annual precipitation is about 750 mm (max November 101 mm, min July 51 mm) and the mean annual temperature is 12.7° (max July 23.4°, min January 1.3°). The mean annual discharge at the gauge station of S. Quirico, the closest to the river mouth, is of 31 m³s⁻¹.

3. Methodology

In this study, GRASS (Geographical Research Analysis Support System), a Free Software/Open Source GIS released under GNU General Public Licence, have been used (GRASS Development Team, 2014; Neteler and Mitasova, 2008). In addition to data digitization, display and georectification, GRASS has been used for the automatic calculation of the channel parameters and their graphical representation through a number of shell scripts.

3.1. Data sources

Of the nine data sources used in this work, the first three (1828, 1881, 1958) required to be rectified and georeferenced. As base map for co-registration we used the very detailed 1976 map images with a resolution of 0.635 m. The Cartographic Office of the Emilia Romagna Region claims for these images high dimensional conformity and isotropy and a negligible georeferencing error due to a scan at 800 dpi and to the use of at least 25 GCPs in georectification for each map sheet. For co-registration we used a minimum of 25 GCPs that could be precisely identified on each couple of temporal images. We selected the GCPs' along both sides of the channel, external to and not too far from it, considering that a better accuracy may be obtained by concentrating the points near the features of interest (Hughes et al., 2006). A second order polynomial transformation matrix was adopted and for cell values resampling the "nearest neighbour" interpolation method was chosen. The positional accuracy was estimated by RMSE. As georectification has been carried out for each single image, different RMSE's have been obtained for the different images of the same date. The highest single image RMSE has been applied to all the images of a specific date. Adopting the United States National Standard for Spatial Data Accuracy methodology (FGDC, 1998) for estimating the Positional Accuracy of points at 95% confidence level (corresponding to a Circular Error at 95% confidence level, or CE95), the RMSE have been multiplied by 1.7308 assuming that the error is normally distributed and independent in each the x- and y-component.

The other datasets are available in georectified and georeferenced form. As reported in each specific related documentation, the Positional accuracy (CE95) for each dataset is ≤ 4 m.

The characteristics of the data sources are summarized as follows:

1828 – Historical Regional map at 1:50000 scale in two paper sheets in UTM system. Edited by the Cartographic Office of the “Regione Emilia-Romagna” in 1999 from old maps of the “Ducato di Parma e Piacenza” at 1:86400 scale. Topographic surveys started in 1821. Scanned, imported in GRASS and georectified. Resolution 2 m. Max RMSE 36.1 m. Positional accuracy 62.5 m.

1881 – Maps at 1:25000 scale in five paper sheets. Edited by the Italian “Istituto Geografico Militare”. Scanned, imported in GRASS, georectified and reprojected from Gauss-Boaga to UTM. Resolution 1.6 m. Max RMSE 13.9 m. Positional accuracy 24.1 m.

1958 – Maps at 1:25000 scale in five paper sheets. Edited by the Italian “Istituto Geografico Militare”. Scanned, imported in GRASS, georectified and reprojected from Gauss-Boaga to UTM. Resolution 1.6 m. Max RMSE 8.4 m. Positional accuracy 14.5 m.

1976 – Maps at 1:10000 scale in 15 georeferenced digital files in UTM system resulting from a photographic reduction of maps originally at 1:5000 scale. Edited by the Cartographic Office of the “Regione Emilia-Romagna”. Directly imported in GRASS. Resolution 0,635 m. RMSE 0 m. Used as the base layer for the co-registration of all the other datasets.

1999 – Orthophotos at 1:10000 scale in 15 georectified digital files in UTM system. Distributed by the “Compagnia Generale Riprese Aeree – Parma”. Directly imported in GRASS. Resolution 1 m. Positional accuracy ≤ 4 m. Flight of April 1998-November 1999.

2003 – Orthophotos at 1:10000 scale in 15 georectified digital files from QuickBird satellite images. Directly imported in GRASS. Resolution 1 m. Positional accuracy ≤ 4 m. Flight of March-September 2003.

2006 – Orthophotos at 1:10000 scale in 15 georectified digital files in UTM system. Distributed by the “Compagnia Generale Riprese Aeree – Parma”. Directly imported in GRASS. Resolution 0.5 m. Positional accuracy ≤ 4 m. Flight of June-July 2006.

2008 – Orthophotos at 1:10000 scale in 15 georectified digital files in UTM system. Distributed by the “Regione Emilia Romagna-AGEA”. Directly imported in GRASS. Resolution 0.5 m. Positional accuracy ≤ 4 m. Flight of June-August 2008.

2011 – Orthophotos at 1:10000 scale in 15 georectified digital files in UTM system. Distributed by the “Regione Emilia Romagna-AGEA”. Directly imported in GRASS. Resolution 0.5 m. Positional accuracy ≤ 4 m. Flight of May-June 2011.

Actually, in the considered time interval other maps are available, but they are of no utility in this contest as they were obtained by previous maps by simply updating roads and buildings but not the stream network.

3.2. Computed parameters

The calculation of the planform characteristics by the GIS based shell scripts requires the manual digitization of only two channel features: banks, represented by the top of the scarp delimiting the channel at bankfull stage, and longitudinal bars, including islands. Just for completeness, also the lateral bars were digitized even if they don't enter in the calculation of any of the considered parameters. The entire digitization process was carried out by the same couple of operators acting in concert in order to reduce the degree of subjectivity.

In order to have reference points fixed in space and time to which refer the channel characteristics and changes from date to date, a unique set of 57 points was digitized along both borders of the channel on the 1976 map. These points are projected perpendicularly to the channel centreline and reported along the x-axis of the graphics of each date with their reciprocal distances and the cumulative distances from the origin.

Many different morphometric parameters and indexes to quantify changes in channel morphology have been proposed by various authors since a long time. Some of them demonstrated to be more effective for a quantitative analysis of historical channel changes. In this study the following indexes and parameters have been computed.

Channel length. This is the length of the channel centerline, or axis, that is the line equidistant from the two banks. In most works the channel centerline is traced manually. In a few works, specific algorithms have been proposed to automatically derive this feature by thinning pixel by pixel a raster map of the channel (Fisher et al., 2013; Pavelsky and Smith, 2008) or to extract it from the bank lines in vector form using Delaunay triangulation principle (Haiyong and Lihong,

2009). In Lauer (2006) the centreline is defined by joining a set of evenly-spaced points along the river channel which equidistance from the two banks is defined by successive approximations. In the present work the centerline is extracted from the vector map containing the river banks by using the modules available in GRASS and especially the module that traces lines parallel to existing features. Starting from the bankfull channel margins, pairs of lines parallel to the channel banks are repeatedly traced toward the channel center. Since each of the two parallels is equidistant from the pertaining bank line, their intersection define points equidistant from the banks. The line joining these intersection points defines the channel centerline.

Channel width. This is the length of the line from bank to bank orthogonal to the channel centerline. In the above mentioned algorithms (Fisher et al., 2013; Pavelsky and Smith, 2008) the channel width is automatically computed along the lines orthogonal to the pixels forming the computed raster centerline. In the present work, a number of regularly spaced transects across the channel and orthogonal to the previously computed centerline are traced by a specific module of GRASS. The length of the transect portion between the channel banks defines the channel width. In order to detail the width variations and considering that the operation is completely automated, a short transect interval of 20 m along the centerline was adopted. A total of about 2700 width values were computed for each channel.

Braiding Index. Among the many different indexes proposed by various researchers to express the degree of braiding (Thorne, 1997), the channel count index of Ashmore (1991) is the most commonly used. It is simply expressed as the number of active subchannels along a channel transect. It is easy to compute and it is the least sensitive to river-stage effects (Egozi and Ashmore, 2008) even though it is anyway affected by a certain degree of uncertainty, both in the maps, for the different scales and for the different interpretations of different cartographer(s), than in the aerial photographs for the different stages at the time of flight. In the present study this index is computed along the same 20 m spaced transects where the channel width is defined.

Sinuosity Index. It is generally defined as the ratio of channel length to valley length (Schumm, 1963). In its classical formulation it requires a prior subdivision of the river valley in rectilinear segments. Then the length of the channel centerline encompassed in the valley segment is divided by the length of the valley segment. The valley segmentation introduces a certain degree of subjectivity especially where the valley shows a curvilinear path. To reduce the degree of subjectivity and obtain a more detailed description along the entire channel development (course?), the sinuosity in this study has been calculated by considering a portion of the channel centerline with a fixed length, progressively shifted downstream of a constant distance. Sinuosity is obtained by dividing the fixed length of the centerline tract by the straight-line between its endpoints. The

value is assigned to the midpoint of the centerline tract. With this procedure the resulting values of sinuosity are strictly related to the value adopted for the constant length of the centerline tract. The maximum possible sinuosity value along a channel is obtained by adopting a fixed length corresponding to the length of the meander with the higher ratio between its length and its neck width. This condition realizes in the channel of 2011 near the river mouth where a meander develops for about 5 km with a neck width of about 200 m. Therefore a value of 5 km was adopted for the constant length of the centerline tracts.

The value of downstream shift of the tracts along the channel centerline is less critical as it simply influences the density of the measures and therefore the detail level and the smoothing degree of the resulting curve. A good detail and a satisfactory smoothing were obtained by adopting an interval of 50 m.

In summary, having adopted a fixed centerline tract of 5 km at 50 m intervals, a total of about 1000 sinuosity values were computed along each channel.

Channell shifting. In many papers (e.g. Gurnell et al., 1994; Leys and Werrity, 1999; Mount and Louis 2005; Bertoldi et al., 2010) the lateral shifting of a channel between two dates is computed as the difference in position of the channel midpoints along sections traced across the floodplain perpendicularly to the flow. As the flow direction changes from date to date and the correspondence between two successive positions of the same centerline point is difficult to assess, in this work a different approach was implemented. The two dates channel centerlines were patched in a unique map and their centerline (or axis), that represents the line equidistant from the two centerlines, is computed following an automatic procedure similar to the previously described procedure adopted to define the centerline between the two channel banks. The distances between the two channel centerlines are then computed along lines orthogonal to the computed axis at regular intervals and are assumed as the channel centerline shifting between the two dates. An interval of 20 m was adopted, the same used for width and braiding calculation. The total mean value was calculated as the average of the shifting values along the orthogonal transects. However, in the case of very small shifting, such as for the short-term intervals where the two centerlines overlap for long stretches, the definition of the centerlines axis with the method adopted resulted impractical and consequently the calculation of the shifting values along the entire channel development was not possible. In these cases, only the total average value has been calculated by dividing the total area included between the two centerlines for the average of their lengths.

3.3. Error assessment

River channel changes quantified from temporal sequences of maps or aerial photographs are valid if the amount of change in the measured parameters exceeds the spatial errors inherent in the source material (Downward et al., 1994). Mount et al. (2003) and Mount and Louis (2005) proposed a number of equations, based on different assumptions, for the evaluation of the error in the measurement of channel width and channel lateral movement (centerline shifting) through temporal sequences of images. In the present work other sources of error needed to be evaluated in consideration of the above described procedure used in defining the centerline position through an iterative tracing of lines parallel to the channel banks and in the peculiar procedure adopted in the centerline sinuosity calculation.

As a whole the error components to be here considered are:

- a) The component connected to the image rectification (residual distortion error).
- b) The component resulting from the imprecision in bankfull identification (ground feature identification error).
- c) The component connected to the deviation of the points along the computed centerline respect to (from?) the true channel midpoint positions.

Assuming that (Mount and Louis 2005):

- a) planimetric errors are isotropic (same imprecision in identifying banks in x and y directions) and invariant (same magnitude for uncertainty in locating both left and right banks);
- b) the distortion image error and the centerline points position error are random (not directional);
- c) the resulting errors for each image date are independent and random relative to those of other image dates (different GCPs have been used for different dates) ;

then, the total error in a single image or between images of different dates can be evaluated using the quadratic sum of the various errors.

On the basis of these considerations, the errors have been evaluated as follows.

1) Error in channel width calculation.

Width calculation is affected by the residual distortion error and by the ground feature identification error for each of the two banks. The total residual distortion error in the two bank positions in a single image (ewd) is:

$$ewd = \sqrt{edb^2 + edb^2} = \sqrt{2} edb$$

where edb is the residual distortion error for each bank defined for each dataset by the Positional accuracy value reported in section 3.1.

The error in identification of the banks in a single image (ewb) is:

$$ewb = \sqrt{elb^2 + elb^2} = \sqrt{2} elb$$

where elb is the error in bank identification assumed to be equal for both left and right banks. The bank identification on a map is generally an easy operation as usually the fullbank scarps are represented (traced, reported ?) by a specific cartographic symbol and the uncertainty in tracing the line along the top of the symbols is negligible (less than one pixel). Problems arise in those tracts where the scarp symbols are not traced and the scarp position have to be interpolated or where many small nearly parallel scarps are reported and a quite arbitrary choice becomes necessary. Also in the photos the top of channel banks can be usually easily detected with a limited degree of uncertainty except where dense riparian tree cover is present. To evaluate the error related to these situations both in maps and in photos, the distance between the selected (adopted, digitized ?) bank line and its most distant plausible alternative position has been measured at points along the entire channel at regular intervals of about 250 m on both banks for a total of about 200 measures. The Positional accuracy at 95% confidence level has been then evaluated and adopted as feature identification error (elb).

The total error affecting bank positions and consequently the width channel calculation in a single image (ew) is given by:

$$ew = \sqrt{(ewd)^2 + (ewb)^2} = \sqrt{2} * \sqrt{(edb^2 + elb^2)}$$

And the total bankfull width difference error between two images of different dates (edw) is:

$$edw = \sqrt{ew_1^2 + ew_2^2} = \sqrt{2} * \sqrt{edb_1^2 + elb_1^2 + edb_2^2 + elb_2^2}$$

where the indexes 1 and 2 refer to the two different dates.

2) Error in centerline shifting calculation.

The error in the centerline position is a further source of error to be added to the error in channel bank positions described above. Therefore the centerline shifting total error (el) for a single image can be estimated by:

$$el = \sqrt{ewd^2 + ewb^2 + ecp^2} = \sqrt{2(edb^2 + elb^2) + ecp^2}$$

where ecp is the error in centerline points position, that is the amount of departure of the points on the computed centerline from their true midchannel position. To define this error, the distances of points on the computed centerline from both banks have been measured orthogonally to the

centerline. As the two distances should be equal if the point is located exactly in the midchannel position, the half of the possible difference between the two distances is the error in centerline position. Also in this case the measures have been carried out at regular intervals of 250 m for a total of about 200 measures along each channel and a Positional accuracy with a confidence interval of 95% has been computed.

The centerline position total error affecting the centerline shifting calculation between two images of different dates (*edl*) is:

$$edl = \sqrt{el_1^2 + el_2^2} = \sqrt{2(edb_1^2 + elb_1^2 + edb_2^2 + elb_2^2) + ecp_1^2 + ecp_2^2}$$

3) Error in sinuosity calculation.

As previously described, in the present work the channel sinuosity is calculated as the ratio between the fixed length of a centerline tract and the distance between the two endpoints of the same centerline tract. So the error in sinuosity calculation correspond to the errors affecting the position of both endpoints (*eep*) and can be evaluated by:

$$eep = \sqrt{ecp^2 + ecp^2} = \sqrt{2} ecp$$

where *ecp* is the error affecting each endpoint position.

The total error (*es*) for a single image can be estimated by:

$$es = \sqrt{ewd^2 + ewb^2 + eep^2} = \sqrt{2} \sqrt{edb^2 + elb^2 + ecp^2}$$

And the total error between two images of different dates (*eds*) is given by:

$$eds = \sqrt{es_1^2 + es_2^2} = \sqrt{2} \sqrt{edb_1^2 + elb_1^2 + ecp_1^2 + edb_2^2 + elb_2^2 + ecp_2^2}$$

To obtain error values comparable with the computed dimensionless sinuosity, *es* and *eds* (in meters) have been divided by 5000 (the assumed constant length of each centerline tract) and named *ess* and *edss* respectively .

The errors resulting by the use of the described equations are reported in Table 1.

4. Parameters calculation and graphs construction

As the calculation of the parameters involve time consuming, tedious and error prone operations, in this work a set of different shell scripts mainly based on GRASS GIS commands was written for

the automatic calculation of the morphometric characteristics and the graphical representation of the results. Only in Lauer (2006) a tool to assist in calculating planform characteristics such as width, curvature, and channel migration at evenly-spaced points along a single-thread river by using manually digitized bank lines is presented. The first script, starting from the digitized features of a specific date, first of all (at first ?) traces out the channel centerline. A number of orthogonal cross sections are then defined at regular intervals along the centerline and both the bankfull width and the braiding index are computed at each section. Finally, the sinuosity is computed at regularly spaced tracts of fixed length downstream along the channel centerline. The output consists in:

- a) a report with the main statistics (see Fig.2 as an example)
- b) a vector map containing the channel centerline
- c) three text files containing respectively the values of channel width, braiding index and sinuosity, computed along the centerline

JOB NAME: Taro 1976

INPUT FILE:

Vector map with banks and bars: vect_topo1976_2013_mod

JOB PARAMETERS:

Distance (m) between transects for width and braiding calculation: 20

Length (m) of channel tracts for sinuosity calculation: 5000

Distance (m) between points where sinuosity values are located: 50

OUTPUT FILES:

Channel centerline vector map: centerline_taro_1976

File with width values: width_1976

File with braiding values: braid_1976

File with sinuosity values: sinuos_1976

COMPUTED CHARACTERISTICS

Channel area A (mq) = 11761798.6185508

Centerline length L (m) = 53728.982242

Mean width (m) A/L = 218.91

Total sinuosity = 1.4664

Minimum width (m) = 34.325062 (Section n. 1723)

Maximum width (m) = 869.590516 (Section n. 335)

Mean transect width (m) = 220.081

Minimum sinuosity = 1.015797 (Progressive point n. 168)

Maximum sinuosity = 24.890106 (Progressive point n. 899)

Mean sinuosity = 1.75954

Minimum braiding = 1

Maximum braiding = 10

Mean braiding = 2.14732

Fig.2. Output report for the 1976 channel. The Mean width is ratio between the Channel area and the Centerline length, while the Mean transect width is the mean of the width values computed at the transects orthogonal to the centerline. The Total sinuosity is the ratio between the Centerline length and the distance between centerline endpoints, while the Mean sinuosity is the mean of the sinuosity values computed at the fixed length tracts along the centerline.

Since the Taro River has a braiding pattern with a very low sinuosity in the upper part, and a single-thread pattern with high sinuosity in the lower one, braiding index was also computed for the single upper part and sinuosity for the single lower one. For the channel shifting calculation between two dates, that requires the pre-emptive construction of the two dates channel centerlines, a specific shell script has been constructed by slightly modifying the script for the channel width calculation as the procedure is very similar, as described in Section 3.2. The output consists in a report with minimum, maximum and mean shifting values and in a text file containing the shifting values at 20 meters interval points along the centerlines axis.

The values of the computed parameters for the six medium-term dates and their variations in the temporal intervals are reported in Table 2. The same parameters are reported for the short-term dates from 1999 to 2011 in Table 3.

dates	1828	1881	1958	1976	1999	2011
years interval		53	77	18	23	12
channel length (m)	46521	49512	53183	53729	53604	54313
length variation (m)		2991	3671	546	-125	709
yearly length variation (m)		56	48	30	-5	59
mean channel width (m) A/l	635	526	286	219	157	172
width variation (m) A/l		-109 [error]	-240	-67	-62	15
yearly width variation (m)		-2.06	-3.12	-3.72	-2.70	1.25
section width (m) min	45.62	37.31	23.17	34.33	33.50	24.31
max	1828.32	2046.63	972.46	869.59	552.80	830.91
mean	640.52	533.59	287.17	220.08	157.32	173.15
braiding index min	1	1	1	1	1	1
max	12	9	8	10	5	8
mean	2.64 (3.83)	2.44 (3.54)	2.31 (3.25)	2.15 (3.62)	1.50 (2.10)	1.72 (2.52)
sinuosity min	1.01	1.02	1.02	1.02	1.03	1.03
max	2.27	5.29	23.20	24.89	24.03	26.54
mean	1.25 (1.61)	1.42 (2.01)	1.74 (2.41)	1.76 (2.42)	1.76 (2.42)	1.78 (2.47)

mean shifting centerline (m)	146 [error]	121	37	36	27
yearly shifting variation (m)	2.76	1.57	2.06	1.57	2.25

Table 2. Computed parameters for the six medium-term dates. The mean braiding index in brackets refers to the channel upper part only, the mean sinuosity in brackets refers to the channel lower part only.

dates	1999	2003	2006	2008	2011
years interval		4	3	2	3
channel length (m)	53604	53655	53941	53961	54313
length variation (m)		51	286	20	352
yearly length variation (m)		13	95	10	117
mean channel width (m) A/I	157	170	153	152	172
width variation (m) A/I		13	-17	-1	20
yearly width variation (m)		03:25	-5.67	-0.5	6.67
section width (m) min	33.50	28.10	19.09	23.15	24.31
max	552.80	608.96	703.98	680.20	830.91
mean	157.32	170.32	153.81	152.34	173.15
braiding index min	1	1	1	1	1
max	5	9	6	5	8
mean	1.50 (2.10)	1.60 (2.31)	1.65 (2.59)	1.54 (2.54)	1.72 (2.52)
sinuosity min	1.03	1.03	1.03	1.03	1.03
max	24.03	24.35	27.01	26.08	26.54
mean	1.76 (2.42)	1.76 (2.42)	1.77 (2.46)	1.77 (2.46)	1.78 (2.47)
mean shifting centerline (m)		10	11	6	15
yearly shifting variation (m)		2.50	3.67	3.0	5.0

Table 3. Computed parameters for the five short-term dates. The mean braiding index in brackets refers to the channel upper part only, the mean sinuosity in brackets refers to the channel lower part only.

The other shell scripts construct graphics in Postscript format showing the curves of the values of width, braiding, sinuosity and shifting computed along the entire channel and saved in the four text files produced by the two scripts previously described. **Single or multiple curves for the different dates can be produced for width, braiding, sinuosity and shifting.** In addition to the curves of the original computed values, curves of simple moving average of various orders can also be drawn. For width, braiding and shifting, calculated at 20 m intervals, many different moving averages has

been experimented. A moving average of 21 terms, embracing a 400 m centerline portion, revealed (turned out?) to produce a good smoothing of the detailed original values producing curves easier to analyse and compare. The sinuosity curve presents a certain degree of smoothing due to its construction method (procedure ?) and no averaging was necessary.

The curve of each single parameter (width, braiding, sinuosity) was constructed for each of the 9 dates considered in this work for a total of 27 graphics. Furthermore, considering that the object of the present work is the analysis of planform changes in time intervals, graphics containing the curves of each parameter, including channel shifting, have been constructed for each couple of subsequent dates. Finally, for a handy overview of the progressive variations of the channel characteristics in time, the curves of all dates for each single parameter have been drawn together in a single graphic.

In order to produce detailed graphics we adopted horizontal scales ranging from 1:30000 to 1:50000 resulting in more than 1 meter long graphics. Examples of single and multiple graphics can be found in the supplementary material.

5. Analysis of the results

5.1 Channel changes

In the following sections, the planimetric changes between couples of dates will be analyzed. To help in the analysis, two graphics have been constructed: in the first one the bankfull limits with subchannels and the computed centerlines are reported for each date; in the second one the four types of curves described in the previous section have been assembled in a simplified form and at reduced scale for each temporal window. For simplicity, only the 21 terms moving average curves are reported for width, braiding and shifting. The values of the computed parameters discussed in the following descriptions are reported in Tables 2 and 3. Only the parameter changes greater than the errors reported in Table 1 will be deemed to be significant and worthy of being analyzed and discussed.

In the attempt (In pursuit of) to estimate the relationship between the channel changes and the various controlling factors, the available information on the hydrological characteristics and the different types of anthropogenic activity have been collected. In Fig. 3 the stations located in the Taro basin and the related recording periods are listed. Discharge values are available at five gauging stations and stage values at eight stations located along the channel, from the highest, S. Maria, to the lowest, S. Quirico. The data are discontinuous and measures started on 1923. Many more (67) are the rainfall stations distributed in the basin of the Taro River with records since 1914.

We selected eight of them based on their location (Fig. 1), the quantity and temporal continuity of the recorded data.

Fig.3. Hydrological data at the gauge stations in the Taro River basin.

The Taro River is heavily impacted and many channel conditioning works have been carried out over the last 200 years. Starting from 1816 as many as 10 bridges crossing the study reach have been built. The river is crossed by two railway lines, by the first and most important Italian motorway (E35) and flanked for a length of about circa 20 km by a more recent motorway (E33). Channelization works currently affect the whole water course, except for a stretch (tract?) of about 20 km in the upper part of the study reach where it has been recently established (1988) a fluvial park in which the river control works are limited and the stream is partially free to wander.. Descriptions, often detailed, of human interventions have been derived from the rich historical documentation. Since a long time gravel mining is a diffuse practice along the Taro river, as in many other rivers all over the world, but there was a sharp acceleration after World War II , particularly after 1950s, with the towns and infrastructures reconstruction and expansion. Before 1975, the quantity extracted is estimated approximately by several authors on the basis of the direct effects on the works in the river bed.. Quantitative information, even if surely underestimated, on the amount of gravel extracted are available starting from 1975 when the activity was regulated by mining concessions. Due to the increasing damages to protection structures, bridges and environment, since 1986 the in-channel mining is nearly completely prohibited except for small quantities aimed to reduce the hydraulic risk.

5.1.1 Pre-1828

Most of the studies on the channel morphology changes in the European area, agree in recognize an increase of sediment supply and braiding since the Middle Ages, as the result of various concomitant causes linked to human activity and climatic changes, as resumed for example in Gurnell et al. (2009) and in Segura-Beltrán and Sanchis-Ibor (2013). The widespread deforestation and the agriculture expansion, due to the increase in rural population, together with climatic deterioration during the Little Ice Age, increased runoff and sediment supply.

As regards the study area, in Veggiani (1984) a detailed analysis of the historical documentation between the XVI and XVIII centuries concerning the situation of the rivers of the eastern Po plain, is reported. The continuous increase in sediment supply came to block the access to the ports of the Adriatic Sea at the eastern end of the Po plain. The strong aggrading of the Taro River is confirmed by old local maps and by historical documents reporting the need of unceasing works to adjust the

outflow of the artificial (man-made) channels flowing in the main reach to the increasing level of the main riverbed. As for the works along the watercourse is to report the construction, between 1816 and 1821, of the first bridge crossing the river along the “Via Emilia” road, which resulted in a remarkable artificial narrowing of the riverbed, clearly visible in the plan view (Fig. 4) and in the width curve (Fig.5) of 1828 between R18 and R19.

5.1.2. 1828-1881

In this time interval of 53 years the channel length increases of about 3 km corresponding to an average increase of 56 m/y. The channel width reduces on the average of 109 m (from 635 m to 526 m) , that corresponds to a reduction of 2.06 m/y. Also the braiding index decreases from a mean value of 2.64 to 2.44 (from 3.83 to 3.54 in the upper reach). On the contrary, the sinuosity increases from 1.25 to 1.42 (from 1.61 to 2.01 in the lower reach). The shifting of the channel centerline is on the average of 146 m (2.76 m/y).

The computed values testify an inversion in the pre-1828 trend that probably occurs gradually during this time interval, with the end of the climatic deterioration of the Little Ice Age and the increasing of river channelization. However, it is evident from plan view (Fig.4) and curves of the parameters (Fig.5) that the planimetric changes are not homogeneous along the channel. Particularly marked is the narrowing between the reference points R6 and R11 where a wide portion of the left side of the riverbed is abandoned for a length of about 5 km, with a width reduction of about 900 m (50%), with a consequent reduction of braiding from 11 to 3 and a centerline channel shifting of about 800 m. This retreat, which alone justifies the majority of the entire channel narrowing, is surely of anthropic origin as reported in the historical documentation that describes the construction of a channel to reclaim the marshy and unhealthy area and the planting of a vineyard that is clearly reported in the map of 1881.

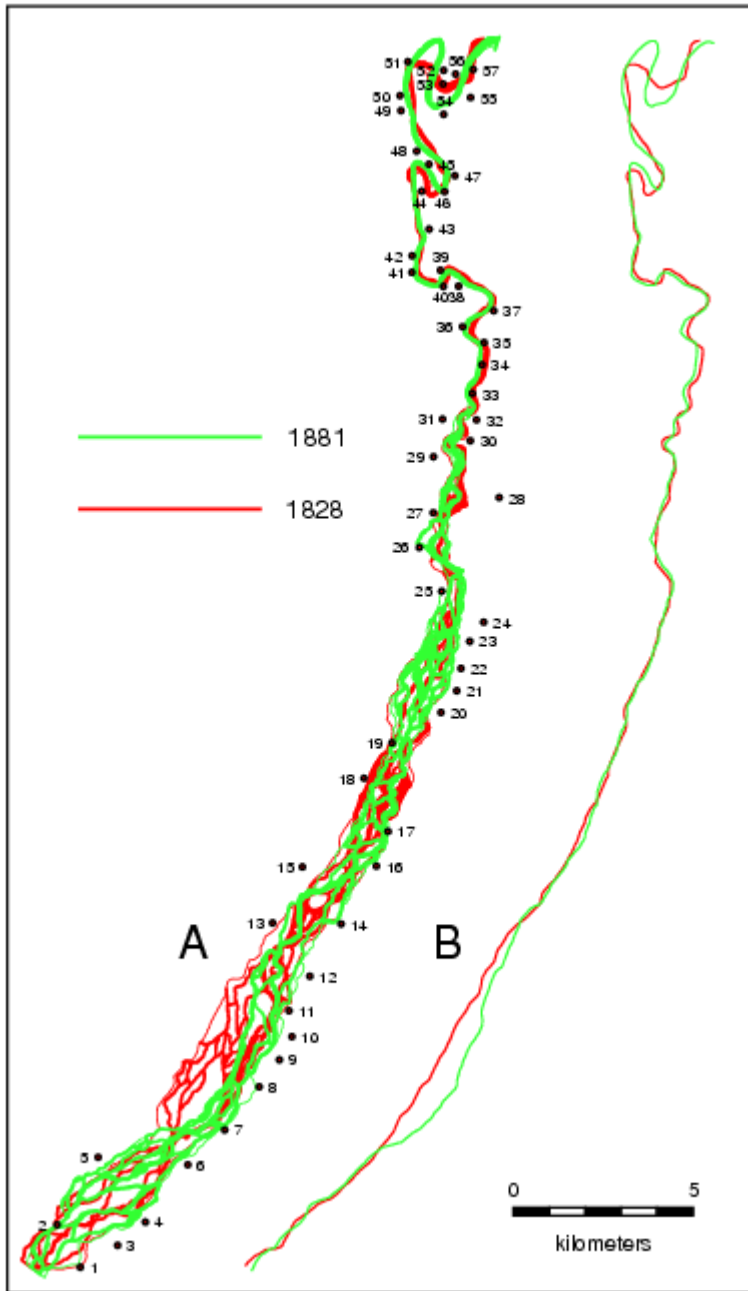


Fig. 4

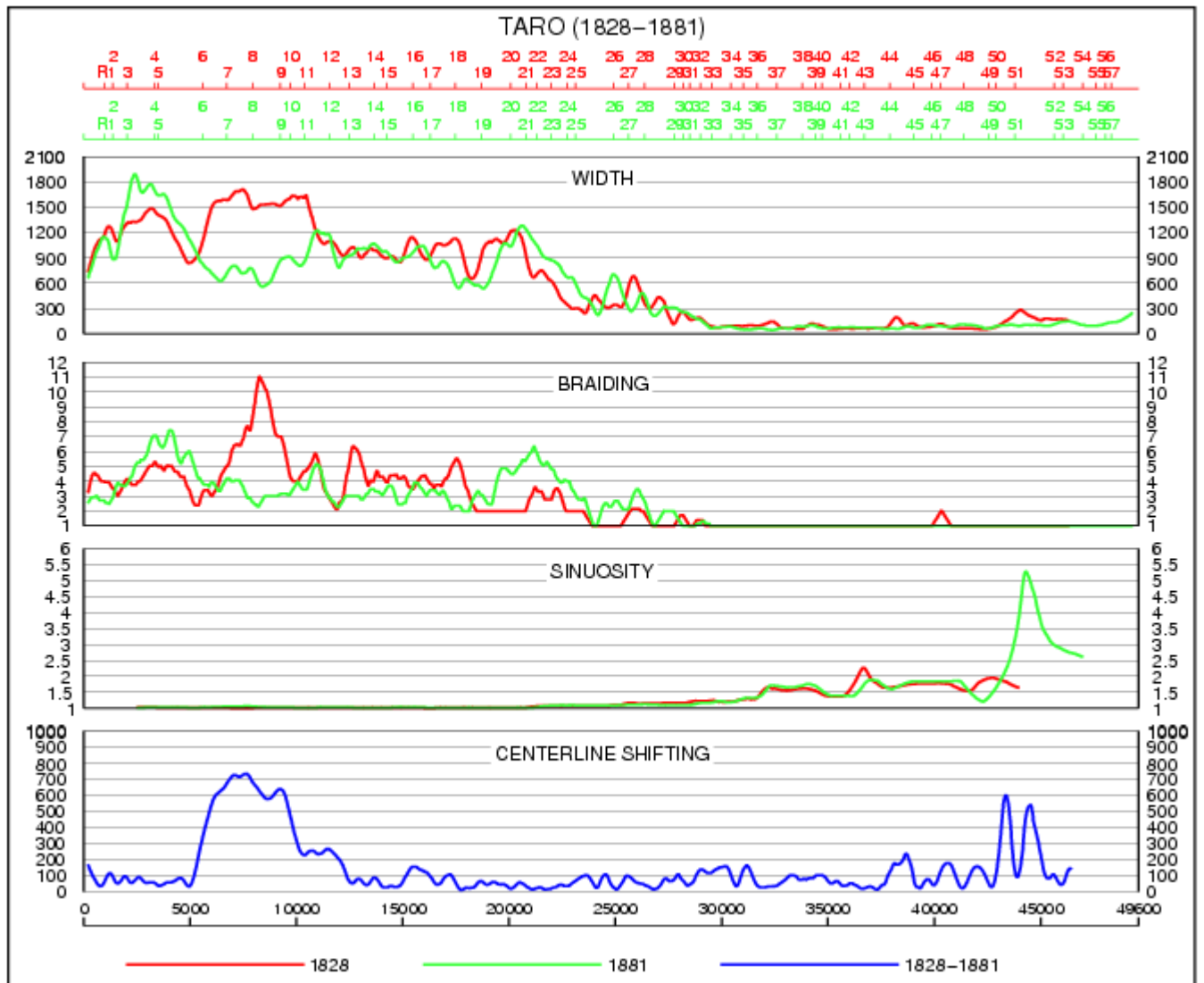


Fig.5

The channel narrowing seems to have led repercussions immediately upstream, between R3 and R6, with an evident increase of width (about 300 m) and braiding.

The construction, between 1851 and 1860, of the bridge of the Milano-Bologna railway immediately downstream of the existing bridge on the Via Emilia, produced a further increase of the already cited narrowing for the construction both up- and down-stream of bank protection structures as apparent in the curve of 1881 between R18 and R19. At the end of these structures, after R20, there is slight channel widening and a marked increase of braiding. To the marked narrowing in the upper part of the reach can be probably ascribed an increase of the erosional capacity of the flow and the consequent elongation of the meanders in the lower portion of the reach. To this meanders elongation is to ascribe the increase of the sinuosity, the high values of centerline shifting and the already cited increase of the channel length of about 3 km.

The gravel in-channel mining is surely moderate, at least at the beginning of this period, due to the limited requirements and to the rudimentary technics of mining and transport. Nevertheless it is interesting to note that in Lombardini (1865) the harmful effects of the even exiguous extractions are described for some rivers of the Po plain and specifically for the Secchia R, located about 55 km East of the Taro R.. Narrowing and deeping of the channel are described and the adoption of a rigid regulation invoked.

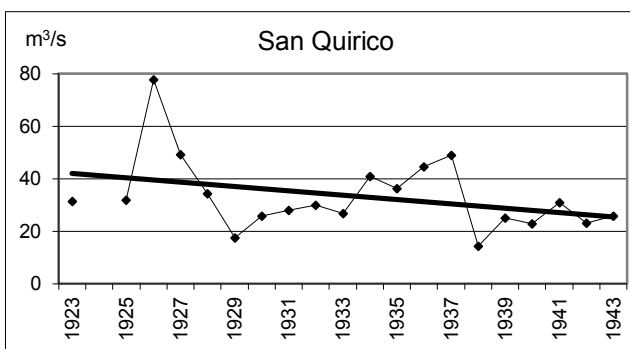
In conclusion, it seems that in this time interval the changes in channel morphology can be substantially ascribed to the human activity both through the subtraction of a wide riveberbed strip and the construction of a bridge with the related up-and down-stream protections. Such activities are surely fostered by the climatic change at the end of the Little Ice Age with the consequent reduction of river discharge and sediment supply.

5.1.3. 1881-1958

In this time interval of 77 years (the longest one) the channel length increases of 3671 m, at an average rate of 48 m/y and the mean channel width reduces of 240 m (3,12 m/y). The braiding average value reduces still further from 2.44 to 2.31 (from 3.54 to 3.25 in the upper reach).

Sinuosity shows a marked increase from 1.42 a 1.74 (from 2.01 to 2.41 in the lower part) that is the maximum increment among the studied time intervals. The mean centerline shifting is of 121 m (1.57 m/y).

In this temporal window discharge data are available for short and irregular periods for the five gauge stations located along the channel. The S. Quirico gauge station, the closest to the Taro mouth, shows the longest sequence, with data from 1923 to 1943. These data show a significant variation from a minimum of 14.3 m³ / s to a maximum of 77.6 m³ / s and a decreasing trend that , however, is strongly influenced by the exceptional events of 1926 (Fig.6A)



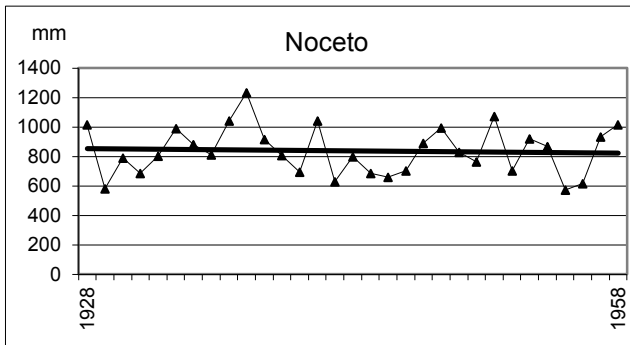


Fig. 6

The other stations, located upstream and with shorter data sequences, don't show clear trends. Also the precipitation data, available for numerous stations and for longer periods, reveal no particular tendencies, as evidenced e.g., by the graph of the Noceto station (Fig. 6B). Since the 1950s, there has been a considerable increase of the in-channel extraction of material in all the rivers of the Apennines as a consequence of the post-war reconstruction and the rapid industrialization and urbanization. In particular the construction of the motorway E35 (Autostrada del Sole), the first and most important Italian motorway, which began in the 1950s, meant a crucial period for the depauperation of the Taro R. (Pellegrini et al. 1979). As shown in the plan view and in the width curve (Figs. 7 and 8) the narrowing affects nearly the entire reach but with different local amounts. The maximum reduction from about 1800 to 600 m, is found downstream R3 where a railway bridge was opened in 1882 and the reach section have been reduced and bank protection structures created (riprap?). Also the later (1905) construction of a bridge at the very beginning of the study reach, upstream R1, resulted in a channel narrowing from about 600 to 300 m. The narrowing downstream of the Via Emilia bridge (R19) as far as the E35 motorway bridge (R25), built in 1957, coincides with an area of heavy sediment mining that caused a remarkable loss of sediment supply and a flow channelization. The consequent greater erosional capacity caused, besides the channel narrowing, a change in the channel typology from braided to meandering between R26 and R29 (Perego, 1994). These changes are obviously clearly reflected in the curves of braiding, sinuosity and centerline shifting. To the increase of the erosional capacity is also to ascribe the further elongation of the meanders at the very end of the reach where sinuosity and shifting show the highest values.

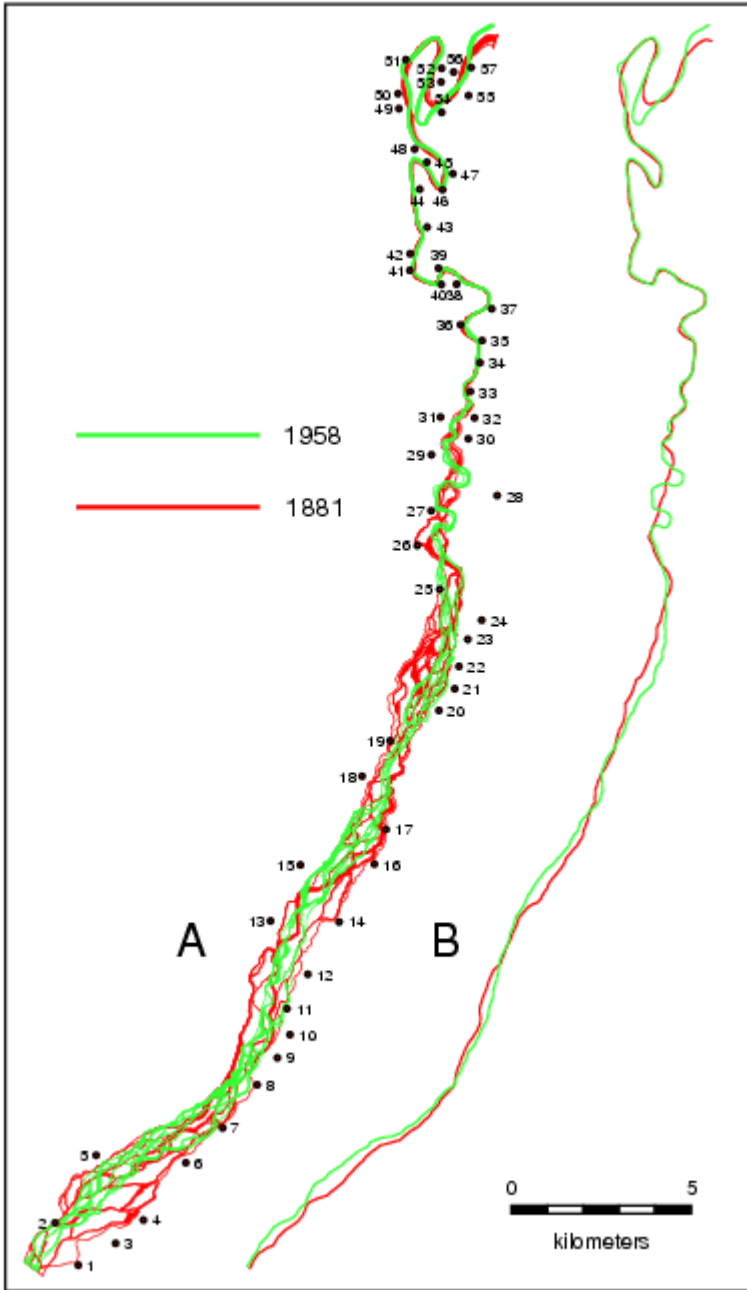


Fig.7



Fig. 8.

The construction of the Gramignazzo bridge, near the confluence into the Po R. (R55), opened in 1936, has not led to a width reduction of the already narrow (≈ 100 m) single-thread channel.

As concerns braiding, it must be considered that in the maps of 1958 is evident a greater graphical detail in the stream network reproduction than in the previous maps. This has surely caused an overcounting of subchannels along the channel transects and an ensuing overvaluation of braiding. This justifies the local increases of the index, as for example between R15 and R17, in spite of the channel width reduction.

In conclusion, in this temporal window, similarly to what reported for the previous period, the morphological changes seem essentially due to human activity, through both the remarkable in-

channel mining and the channelization of long portions of the reach for the construction of three bridges, while the climatic changes seem to be negligible. The higher rate of changes in this time interval for width (from 2.06 to 3.12 m/y) and sinuosity (from 1.25 to 1.42) than in the previous one reflects the broader and more invasive (aggressive) human activity.

5.1.4. 1958-1976

The centerline length increases of 546 m (30 m/y) and the average width reduces of 67 m (3.72 m/y) that is the maximum value of all temporal windows. The mean braiding index for the entire channel reduces from 2.31 to 2.15 (but in the upper portion of the reach it increases from 3.25 to 3.62). The sinuosity shows a slight increase from 1.74 to 1.76 (from 2.41 to 2.42 in the lower part). The mean centerline shifting is of 37 m (2.06 m/y).

The data of river discharge in this short period are scarce; the longest sequence (1959-1974) refers to the uppermost station of S. Maria (Fig.1), that shows a decreasing trend (Fig. 9A). Also the precipitation records confirm a general decreasing, as evident, for example, in the record of the Noceto gauge station (Fig. 9B).

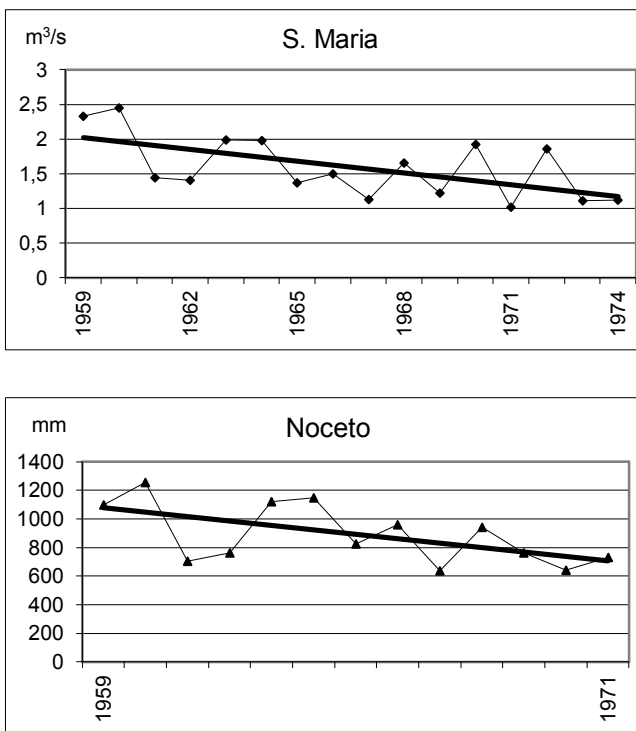


Fig. 9

In this temporal window, much more shorter than the previous ones, there was a maximum of the in-channel mining activity, connected to the accelerated grown of road network and urban constructions. In particular, in 1975 is opened the E33 Parma-La Spezia motorway that borders the

Taro river on the left side for about 20 km. Most of the material used for the motorway construction have been mined from the Taro riverbed. In Tagliavini (1975) the braiding reach of Taro R. is stated as one of the most mined reach of the entire northern Apennines, with 10 gravel crashing plants along the channel (nearly one every 2.5 km). For long stretches of the river the gravel was completely removed, the bed level lowered of 3-4 m and the underlying clayey and sandy deposits deeply downcut. The resulting narrowing affects the entire channel but mainly the upper part with maximum amount between R16 and R26 (Figs. 10 and 11). Furthermore, the map of 1976 reports wide areas isolated and subtracted from the riverbed to position gravel crashing plants, as for example between R16 and R17 and between R24 and R26, on the right river side, whereas the narrowing between R19 and R24 is due to the construction of the great “CePIM” Freight Village covering a surface exceeding 2.5 km² and partly built on the left belt of the 1958 riverbed for a length of about 2.3 km and a width of about 300 m. These large asymmetric occupation of the riverbed are clearly registered by the three central peaks in the shifting curve.

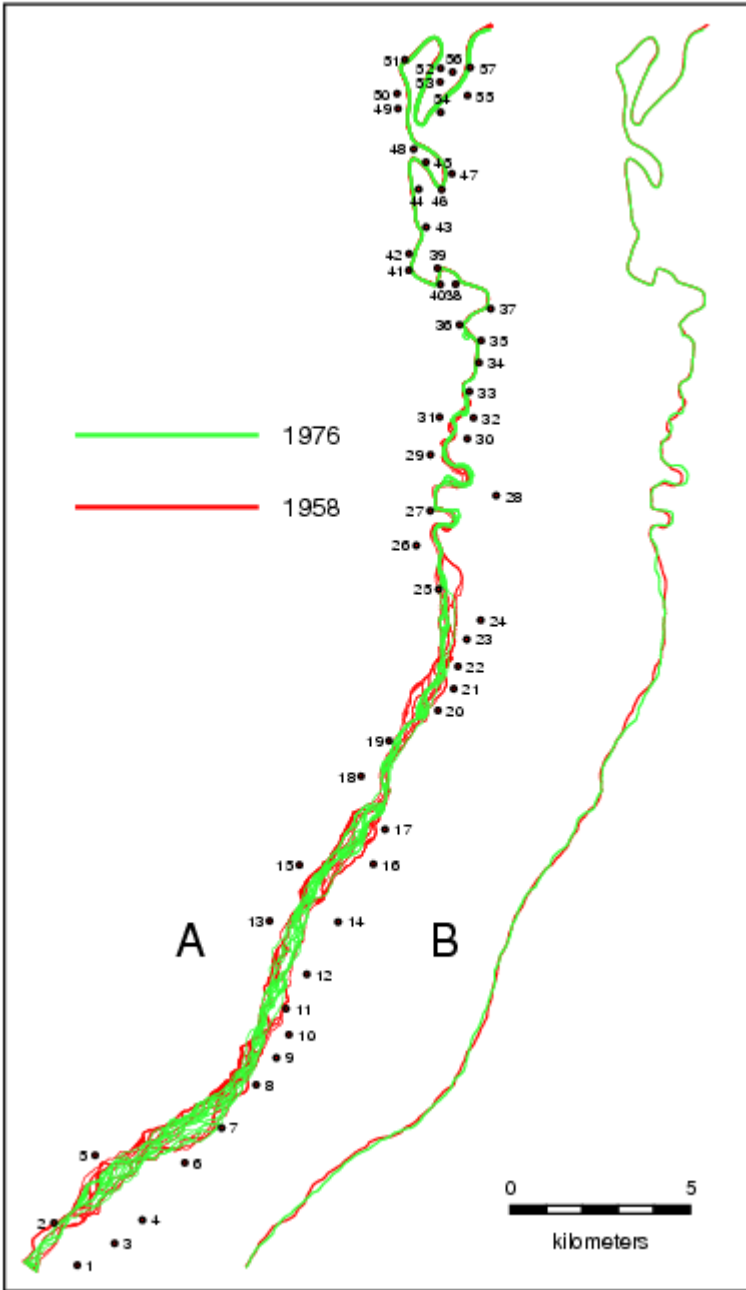


Fig. 10.

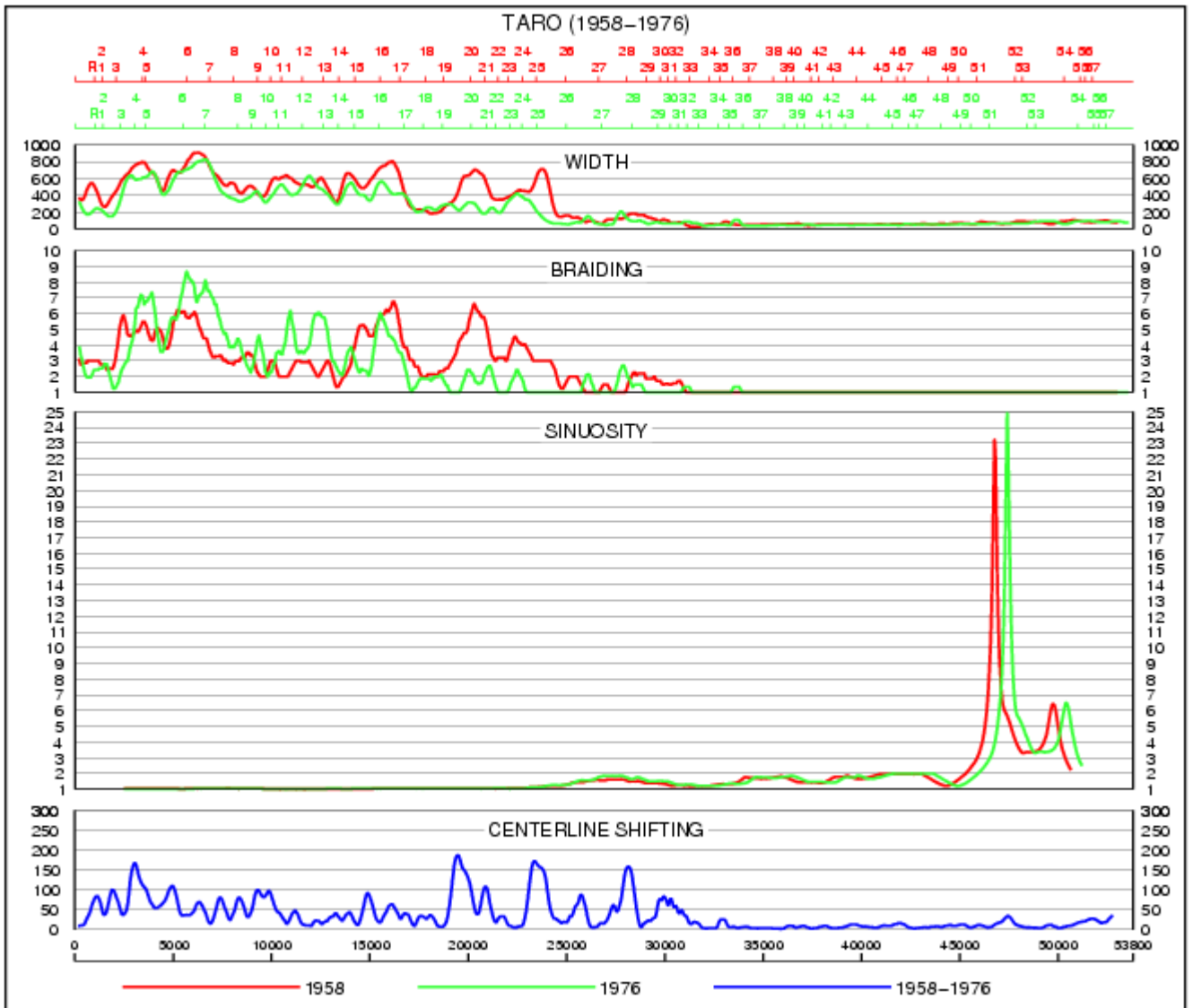


Fig. 11.

As regards braiding, it must be noted that in the map of 1976 at 1:10000 scale the channel network is reproduced with a greater detail than in the map of 1958 at 1:25000 scale, with a consequent increase in the computed braiding values. This “graphical” increase actually affects the upper part of the channel (from 3.25 to 3.62), where the width undergoes minimal changes, while in the intermediate part, subject to greater excavation and to a greater width reduction, also the braiding undergoes a drastic reduction. The slight increase in sinuosity is due essentially to a slight accentuation of the meanders between R26 and R29 which also justifies the increase of the channel length, partly offset by a mouth retreat of 120 m.

It seems evident that the changes in the computed planimetric parameters, and especially the marked width reduction, are mainly the result of the recurrent anthropic subtraction of wide portions of the riverbed for facilities constructions, and partly by the high mining activity. These factors surely overcome the effects of the recorded discharge and precipitation reduction.

5.1.5. 1976-1999

The overall length decreases of 125 m (5 m / y) while the average width is further reduced of 62 m. Braiding reduces from 2.15 to 1.50 (from 3.62 to 2.10 in the upper part) which is the more consistent reduction in all the time intervals analyzed, although it should be considered that the different types of image (maps and ortophotos) can have influenced, at least in part, the reduction in subchannel density. The two sinuosity curves overlap almost perfectly reflecting no significant changes, as confirmed by the identical values of the overall mean sinuosity (1.76) and of the sinuosity of the lower part only (2.42). The mean displacement of the centerline is 36 m (1.57 m/y), one of the lowest among the examined intervals. For this period there are no discharge data, whereas the rainfall record still show a declining trend, as shown in the graphics of Borgotaro and Ramiola stations (Fig. 12).

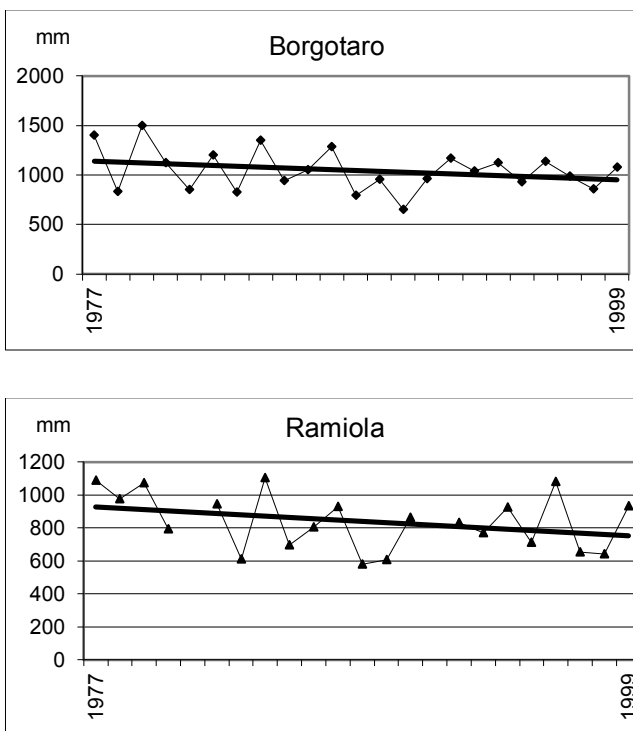


Fig.12

The in-channel mining continues with a fast pace until 1986 when, in order to stop the serious consequences related to mining, a law that drastically limited such activity was issued. Until that date the channel continues to be affected by visible signs of deepening as described in Bizzarri and Terzi (1984), who measured, in correspondence with 9 cross-sections in the reach between Fornovo

(R1) and the Via Emilia (R19) (Fig. 13), a mean decrease of 1 m and locally of 3-4 m in the period 1972-1980. In the same paper the volumes of the in-channel extracted gravel as derived from official permissions are reported: in the period 1975-1981 in the whole Taro River the volume range from about 55000 to 400000 m³/y. The data for the sole study reach that we have collected from public agencies, give annual values ranging from 55000 m³ in 1975 to 274190 m³ in 1985 with a maximum of 433050 m³ in 1978. These data are partial and incomplete and represent surely only a small portion of the volumes actually extracted.

In this temporal window, and especially after the great flood of November 9th 1982 that damaged many bridges and structures, the river was object of heavy interventions such as the raising of embankments, the construction of bank protections, groynes and weirs downstream the bridges to avoid the undermining of piers (Cati, 1984).

Regarding the causes of the planimetric changes, it should be noted that the narrowing interests, even if in a discontinuous manner, the whole upper part of the channel with values of the order of hundreds of meters. However, from the width, braiding and shifting curves (Fig. 14), it is evident that the highest narrowing coincides with the reach portions where riverbed strips previously subject to mining have been abandoned and colonized by a dense vegetation, as in tracts R3-R7, R12- R17 and R22 -R25 on the right side, and between R12 and R13 on the left side. So it seems that even in this time interval the narrowing is essentially connected to the removal of large marginal areas of the riverbed, although it must be considered that the mining activity, which continued until the middle of this time interval, has certainly contributed to a deepening and a narrowing of the channel. To the drastic reduction of the mining activity could be attributed the decrease of narrowing rate from 3.72 m/y of the previous interval to 2.70 m/y.

The absence of changes in sinuosity is the result of the channelization works which have virtually fixed the channel position in the lower part of the reach. The reduction of 125 m in length, the only case of a reduction in all the analyzed time intervals, is mainly due to the withdrawal of the confluence into the Po R. and only in small part to a slight reduction in the curvature of the meanders in the intermediate part of the channel (between R26 and R33).

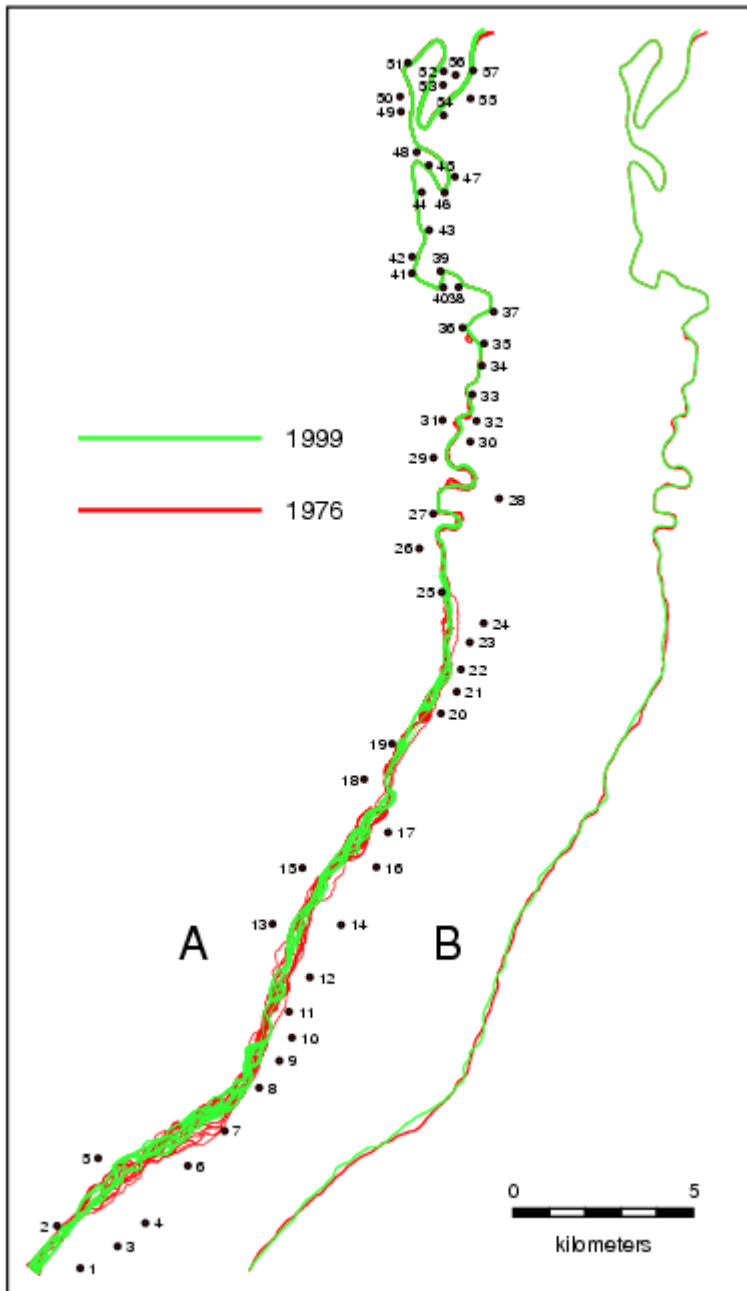


Fig. 13

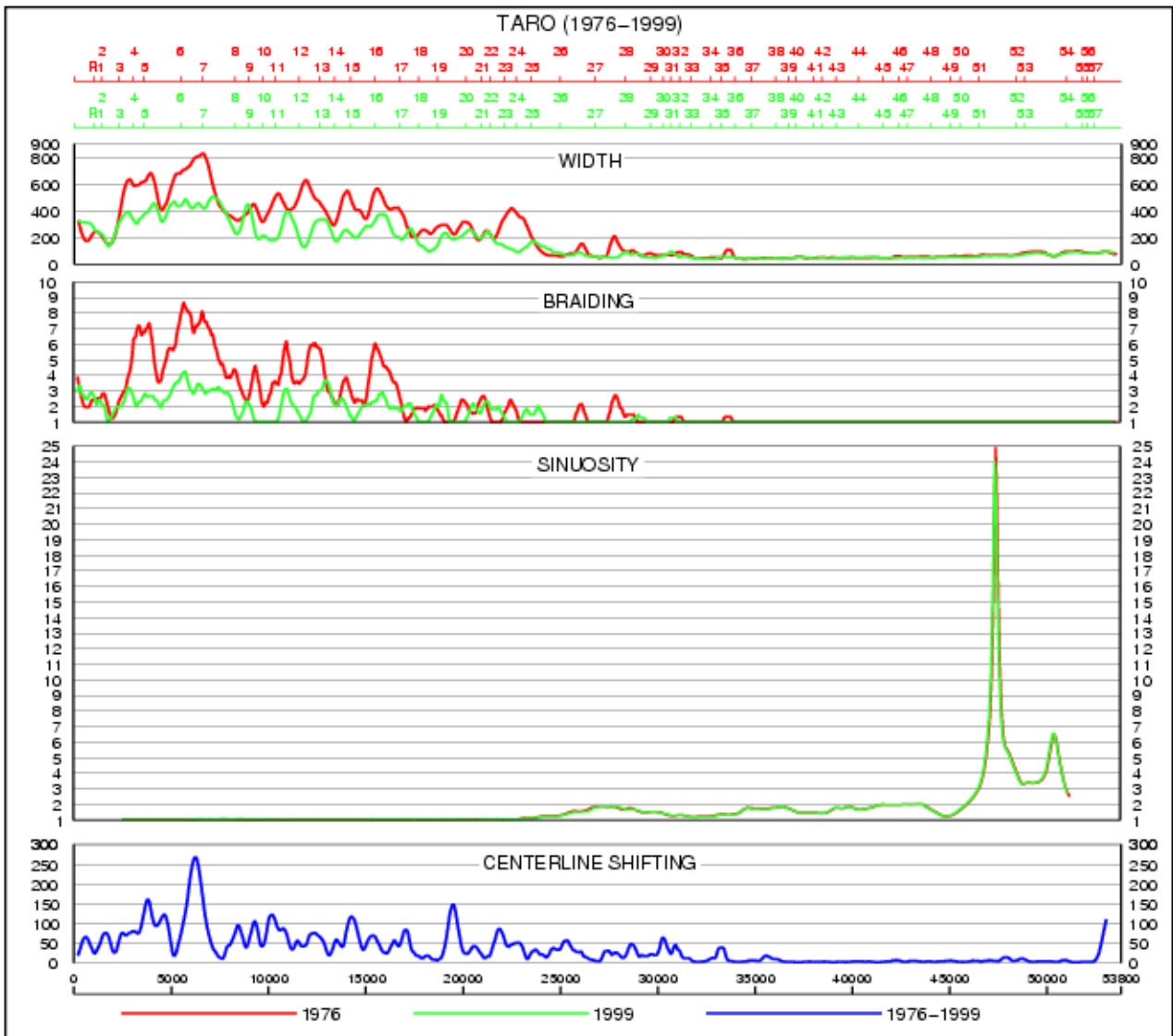


Fig.14

5.1.6. 1999-2011

The length shows an increase of 709 m that represents the more pronounced annual increase (59 m/y). The mean width increases of 15 m (1.25 m/y), a limited increase but in contrast to the progressive decrease of the past. Even the braiding increases for the first time from 1.50 to 1.72 (from 2.10 to 2.52 in the upper part) and the sinuosity presents a slight increase from 1.76 to 1.78 (from 2.42 to 2.47 in the lower part). The shifting is 27 m (2.25 m/y).

For this short time interval the discharge data are available only from 2004 and show a growing trend, largely conditioned however by the great floods of 2000 and 2009 which affected the Taro River and all the rivers of the region, as recorded for example at the Pontetaro station (Fig. 15).

This is confirmed by the stage values recorded at the S. Quirico station that reached 15.60 m and 14.44 m for 2000 and 2009 respectively, against an average of 8.59 m in the previous 50 years and exceeded only by the 15.80 m of the flood of 1982.

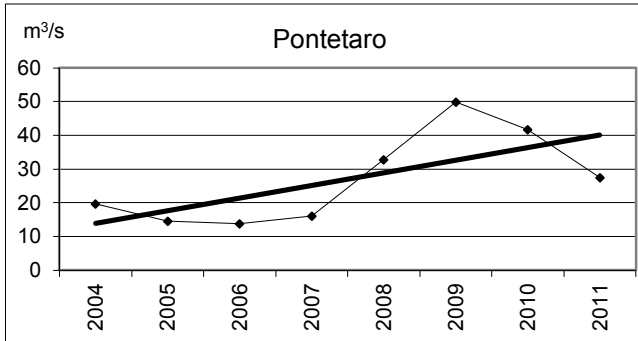


Fig.15

As clearly shown in the plan view of Fig. 16 and even more in the curves of Fig. 17, the width rise affects most of the upper part of the reach with values up to 300 m. in parallel with the braiding increase. The sporadic narrowing are located in correspondence of two new bridges built in 2004 (immediately upstream of R20) and in 2008 (between R11 and R12) respectively. It is worth noting that the changes in the average width calculated separately for the upper and lower parts of the reach give a widening from 273 to 304 m in the upper part and a slight narrowing from 63 to 57 m in the lower one.

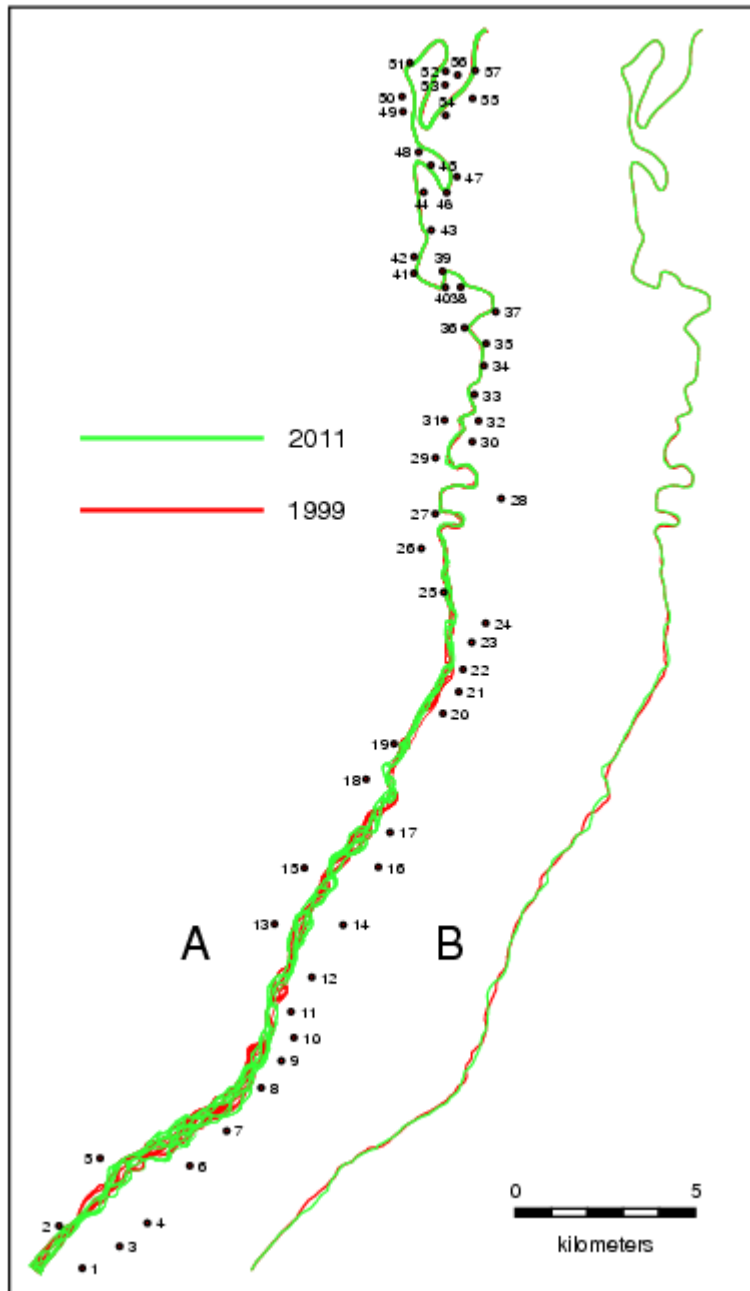


Fig. 16

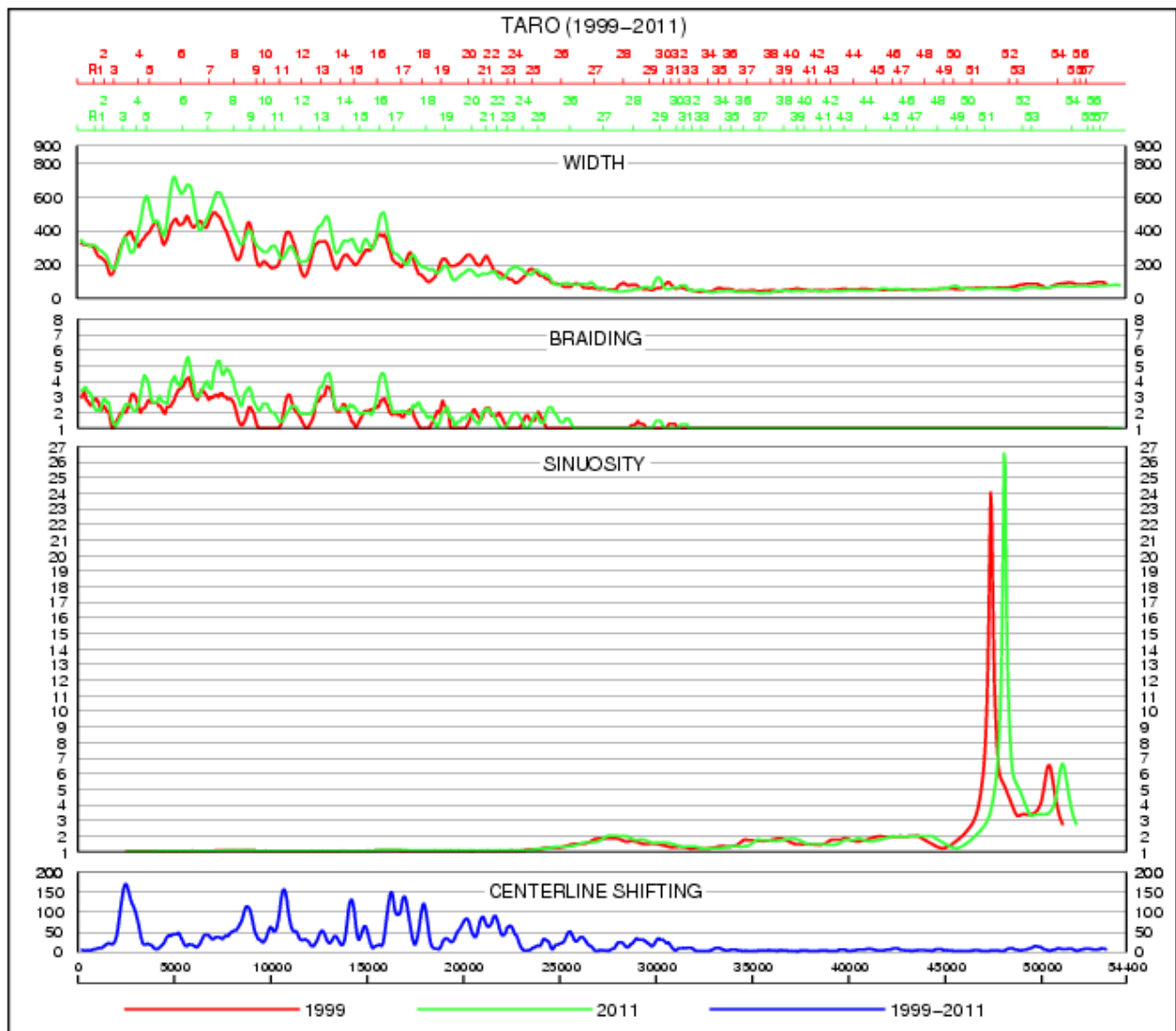


Fig.17.

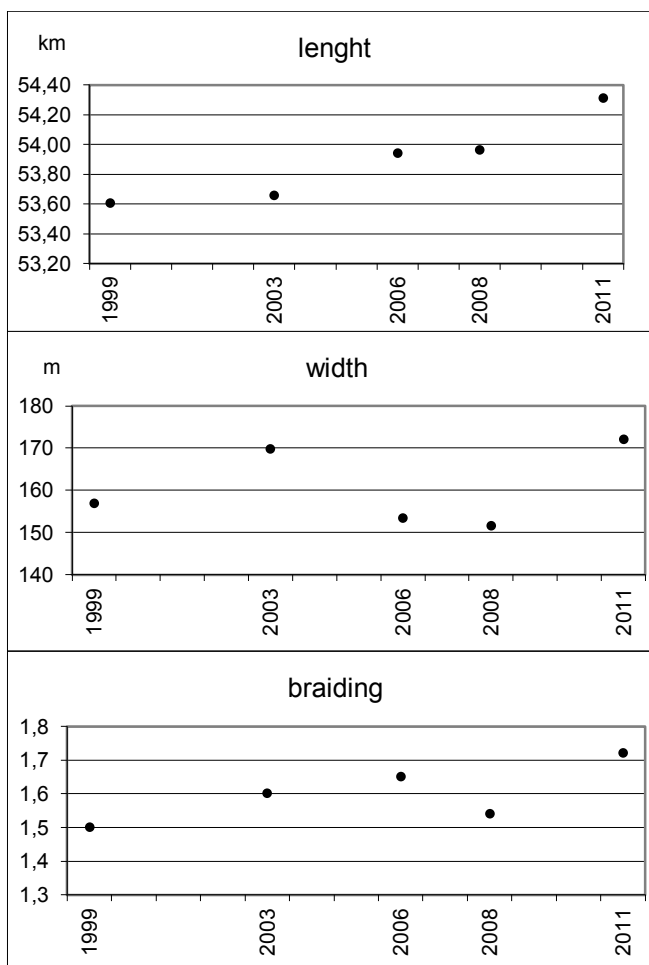
The differences between 1999 and 2011, are obviously the result of discontinuous and sometimes conflicting variations that have occurred along the time interval considered.

The availability of data for some intermediate years allows to evaluate the changes of the parameters on short time intervals and evaluate the effects due to occasional events that involve temporary changes in river morphology. In this short-term analysis the curves of the parameters values along the entire channel development are of limited utility due to the very small changes along most of the channel which magnitude a cause della limitata entità dei changes lungo la maggior parte of the channel la cui magnitude is often close to the magnitude of the estimated errors. Only the width curve of 2011 shows a clear and significant increase in some portions of the upper part of the channel (Fig. 6-S in the supplementary material). In the braiding curves (Fig. 7-S in the Supplementary material) significant changes appear more difficult to assess and in the sinuosity curves changes appear negligible (Fig. 8-S in the supplementary material). On the

contrary the mean values of the parameters show changes that, although limited, allow to make some consideration (Table 3, Fig. 18).. In this analysis the changes although these assessments involve a certain degree of uncertainty as the magnitude of the measured changes is often close to the magnitude of the estimated errors. In such a circumstance it seems more useful to evaluate the overall changes by comparing the mean values of the various parameters

In the short-term analysis (Table 3, Fig. 18) The channel length shows a progressive increase although with different rates: in the period 2008-2011 it shows the greater increase (352 m). The mean width increases from 157 to 170 m between 1999 and 2003, reduced from 170 to 152 between 2003 and 2008 and increases again to 172 m in 2011.

Similarly, braiding reveals alternating changes in the different periods. Sinuosity shows a slight progressive increment from 1.76 to 1.78 in parallel with the progressive increase of channel length, revealing, as expected, be largely unaffected by temporary changes of the river width and braiding. Also the shifting has slight and alternating variations, the highest in the 2008-2011 period.



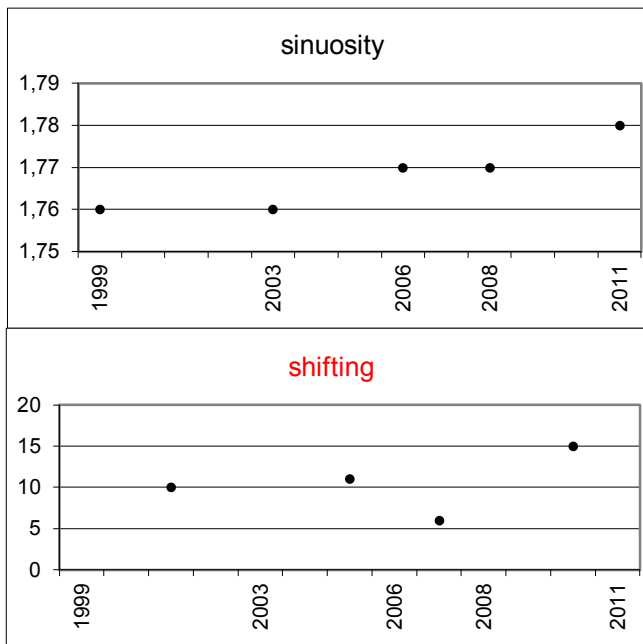


Fig. 18. Values of the computed parameters in short-term periods from 1999 to 2011.

The alternating changes of most of the parameter values seem to reflect temporary and reversible changes in the channel morphology connected to episodic events. In particular, there is clearly a close temporal relationship with the above cited exceptional floods of 2000 and 2009 which effects are also visible in the ortophotos of 2003 and 2011, where are evident strong bank erosion, the reach enlargement and an increase of the number of subchannels that justify the increase both of width and braiding. After 2003, and till 2006, there is a quick recovery of the effects of the flood with a quick width reduction that continues, even if more slowly, till to 2008 and supposedly till the next flood of 2009. Delayed and slower is the reduction of braiding and shifting. The flood of 2009 produces a new consistent increase of the same parameters as registered by the values of 2011. It can be supposed that this last situation be temporary and probably doomed to a return to parameters similar to the previous ones, as happened in the past for the flood of 2000. Length and sinuosity appear rather less conditioned and have simply a more pronounced increase in the periods affected by the two floods. Based on these considerations, the evaluation of morphological changes based simply on the two extreme dates, 1999 and 2011, should be reappraised. In particular, there is not a clearly identifiable evolutionary trajectory toward an increase of the parameters, and it seems more plausible to suppose a maintenance of a steady state in the morphological situation. This consideration appears in agreement with the findings reported by Piegay et al. (2009) for some rivers in France, according to which the recent channel changes may be considered short-term fluctuations related to specific flood events, rather than real long-term adjustments. But it is in

disagreement with most of the works on the Italian rivers in which the recent recovery are considered an effective and permanent return to the previous conditions (see for example Comiti et al. (2011)).

5.1.7. 1828-2011

In the whole time interval of about two centuries, the length of the channel increases of 7792 m (42.6 m/y) equal to 16.7 % , while the average width is reduced of 463 m (2.5m /y) which corresponds to the 73%. Braiding reduces from 2.64 to 1.72 in the entire channel (from 3.83 to 2.52 in the upper part) with the maximum number of subchannels reducing from 12 to 8. It should be considered that this reduction is undervalued as in the recent images, at a scale of 1:10000, the subchannel network is much more detailed than in the historical map of 1828 whose original scale is 1: 86400. Sinuosity changes from 1.25 to 1.78 (from 1.61 to 2.47 in the lower part). The computed average shifting gives a value of 224 m (1.22 m/y).

As evident from the plan view and curves (Figs. 19 and 20), the length increase is largely due to the formation and subsequent development of the meanders in the lower part of the channel as revealed by the increase in sinuosity and shifting. The width reduces mainly in the upper part of the channel in parallel with the reduction of braiding.

As pointed out in the previous analysis of the single temporal windows, the parameter changes are not homogeneous in the considered intervals (Fig. 21).

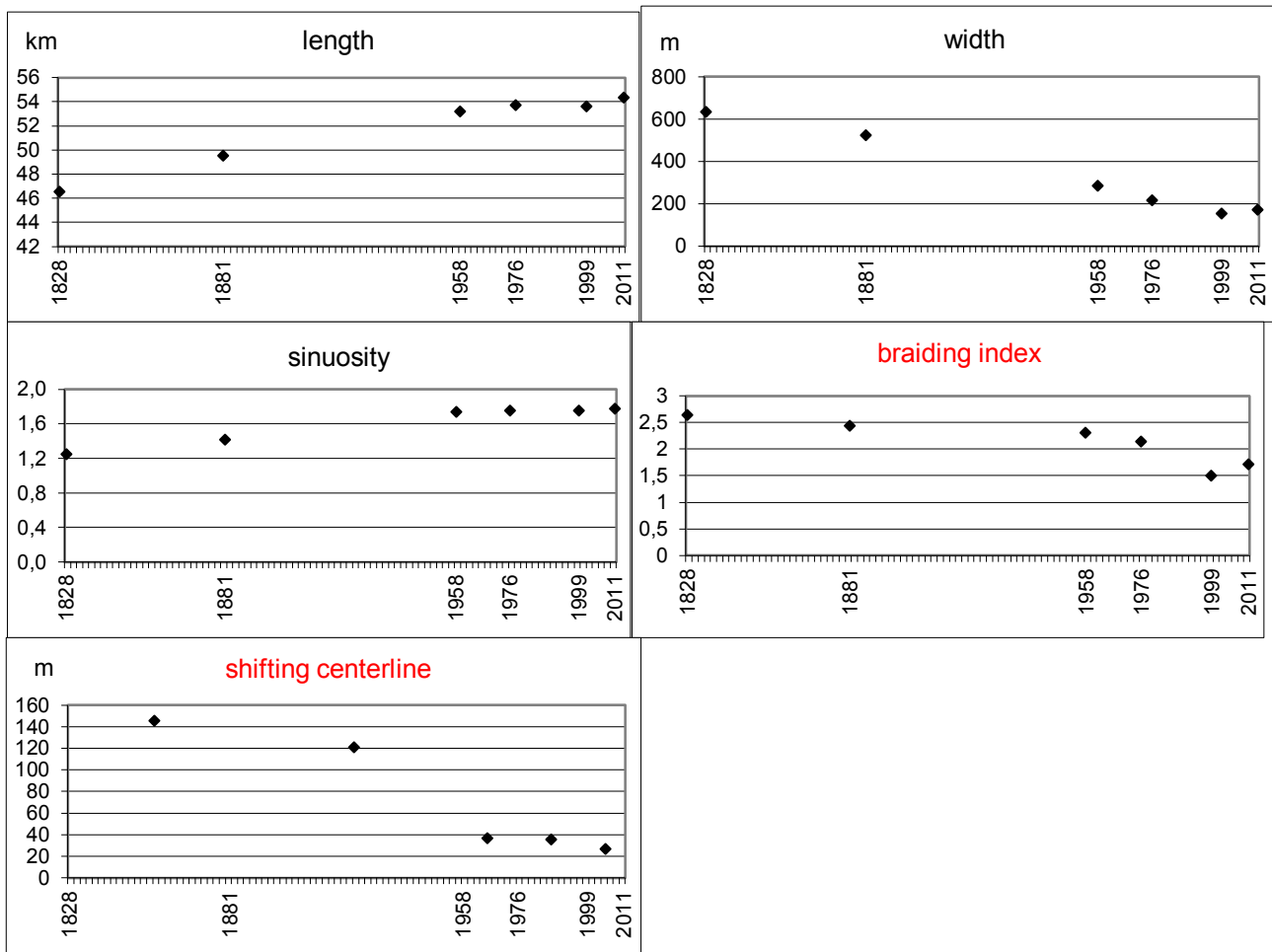


Fig. 21

For example, the length increases continuously, except for a decrease of 125 m between 1976 and 1999 substantially justified by a displacement of the point of confluence in the river Po, as mentioned earlier. It should be noted that until 1976 the elongation is a result of accentuation of the portion of the meandering reach, while from 1976 onwards the meandering portion remains virtually unchanged as a consequence of the numerous protection works and lengthening substantially affects only the upper portion of the reach where the river is partially free to wander inside the Taro fluvial park. The same causes can be cited for the changes in sinuosity, closely linked to changes in length, which increases steadily from 1.25 to 1.76 until 1976, and then with a low gain up to 1.78.

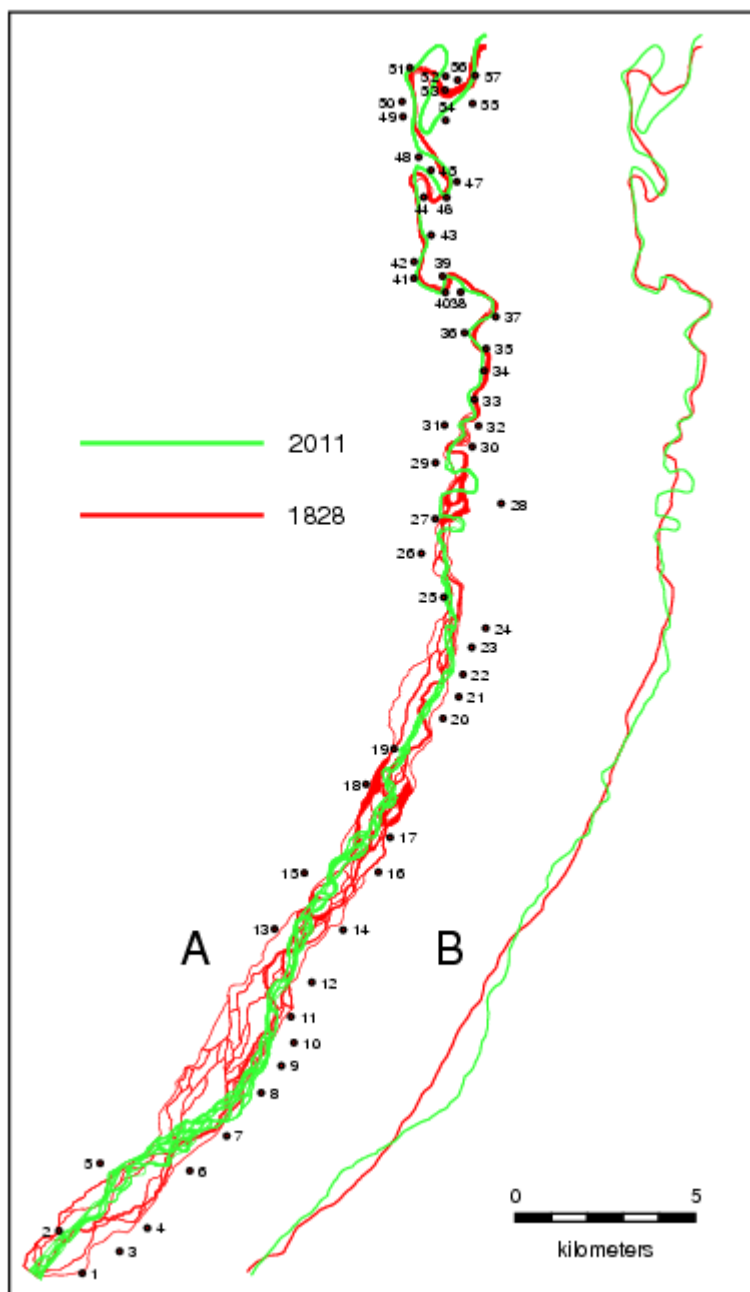


Fig. 19

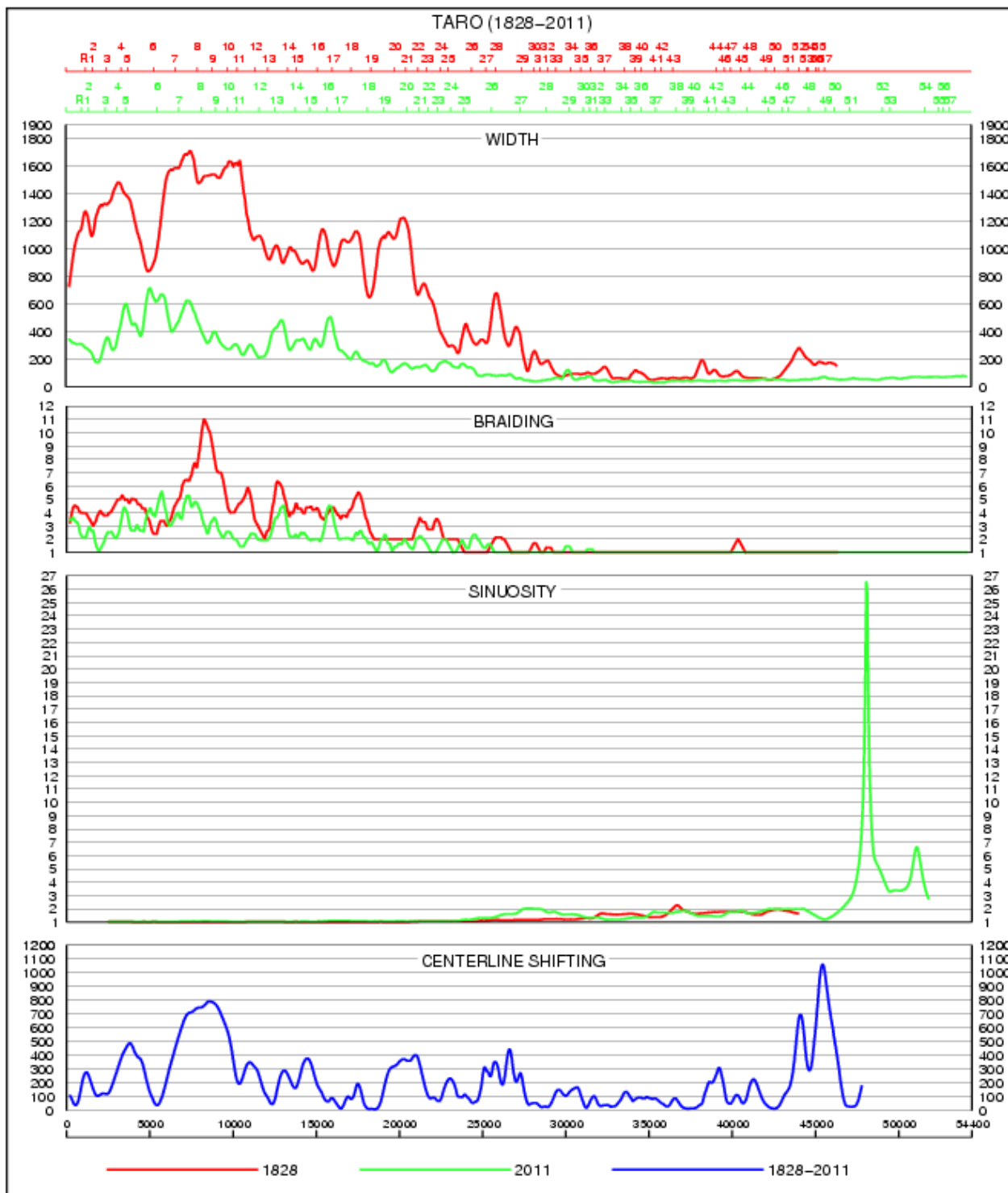


Fig.20.

As regards the channel width, till 1976 the reduction rate increases steadily up to a maximum of 3.72 m /y, then slow down to 2.70 m/y and switch to a modest increase of 1.25 m/y in the last period 1999-2011. However, as already discussed earlier, in the latter period the width shows considerable variability and is strongly influenced by the widening of 2003 and 2011 connected to two exceptional floods.

Braiding shows a slow and progressive reduction until 1958, a rapid decrease in the subsequent period up to 1999 and the already discussed particular increase in 2011.

Shifting shows a gradual decrease of the values in the different time intervals. However, if we consider the different lengths of the intervals, the annual shifting shows high variability with a maximum in the temporal window 1828-1881.

As clearly shown by the position of the two centerlines (Fig. 19), there is no prominent direction of shifting. So the river eastward migration observed for the past and attributed to the particular structural setting, does not seem to have occurred in the last 200 years. On the other hand, as demonstrated in the analysis carried out, the magnitude and direction of the shifting is mainly due to the anthropic activity and any slow tectonic component would be anyway difficult to discern. Although it is difficult to define the contribution of each controlling factor, especially when they act in concert and with different intensity over long periods, it is quite evident that the planimetric variations of the Taro R. till the situation shown in the 1881 map are due almost exclusively to the continuous anthropic removal of wide marginal portions of the riverbed favored by the decrease in precipitation and sediment supply connected to the end of the Little Ice Age.

Since 1881, while continuing the anthropic removal of portions of the riverbed and the relative narrowing of long stretches of the reach, other factors become important. In particular the mining activity and, secondly, the reduction of the river discharge. The increase of the in-channel gravel mining, not offset by sediment supply, and the consequent increased erosional capacity of the flow, resulted in a significant deepening of the riverbed, an acceleration in the rate of narrowing, the accentuation of the meanders in the lower reach and the formation of new meanders in the middle portion of the reach. More recently, i.e. since the situation shown in the orthophotos of 1999, the drastic reduction of mining and the nearly complete channelization of the lower part of the reach, led to a substantial stabilization of the downstream half of the study reach. Only the upper part of the reach, where the channel is relatively free to wander, is affected by limited planimetric changes.

5.2. Comparison with previous works

The morphological changes observed in the Taro R. agree with adjustments observed by other Authors in many Italian and European rivers even if the differences in the temporal windows analysed often hamper a detailed common chronology of the events. Furthermore, in the previous works the analysis is usually limited to width, bed elevation and channel pattern changes while sinuosity and channel shifting are rarely considered, at least in quantitative terms.

Limiting the comparison to the most recent and significant works relative to the Italian rivers, the channel narrowing and incision at increasing rate in time, and the channel pattern modifications

measured in this work for the Taro River, represent a common channel evolution. For example, all the rivers reviewed by Surian and Rinaldi (2003) from Alps to Sicily, in the last 100 years experienced remarkable narrowing (up to 90% in Piedmont Region) and incision (locally up to 12 m in the Emilia- Romagna Region) and many of them a pattern change, usually from braided to transitional. Similar situations are found by Rinaldi (2003) for the alluvial rivers of Tuscany Region (Central Italy) affected by a generalized bed level lowering that reached 9 m in the Arno River and a channel narrowing higher than 50% in the 38% of the measured reaches. The channel pattern changes from multi-thread to single-thread sinuous channel with alternate bars. Pellegrini et al. (2008) studied the morphological changes since the end of 1880s of three multi-thread Po River tributaries, in the Northern Italy, detecting a narrowing up to 80%, a channel incision up to 4 m, a lengthening of the channel axis, and locally a change from multi-thread to single-thread, until the 1990s. In Ziliani and Surian (2012) the morphological changes of Tagliamento River (Northeastern Italy) from 1805 to 2009 have been analysed. After a slight widening of about 4% in the period 1805-1833, a narrowing, with increasing rates, affects the channel till 1990 for a total width reduction of 60%. An average value of 1 m was calculated for incision. The braiding index halved on the entire period even if with different rates. In Rinaldi et al. (2005) the morphological changes that occurred during the last two centuries along the lower reaches of the Trebbia and Vara rivers in the northern Apennines are analyzed. A first phase of narrowing (between 10 and 25%), limited bed incision and reduction of braiding affect both rivers until about the first half of the 20th century. A second phase of more relevant channel narrowing, bed incision (up to 3.5 m) and braiding reduction occurred during the second half of the 20th century. Castaldini and Ghinoi (2008) report for the multi-thread reach of the Panaro River, a Po River tributary, a narrowing of about 390 m (56%), an incision locally up to 9 m and a change from braided to wandering over the last 120 years. For Comiti et al. (2011) the narrowing of the active channel area of the Piave River (North-East Italy) began in the first half of the 1900s after a period of remarkably widening during the nineteenth century, and produced a total narrowing of about 80%, a bed incision up to 2 m and a change from a dominant braided to a wandering pattern. Also in the four rivers studied by Surian et al. (2009) in the same Alpine area the narrowing started in 20th century, after a period of relatively small changes, and produced a channel reduction by up to 76%, an incision by up to 8.5 m, and changes in channel configuration, with a general reduction of braiding and in some reach a change of typology from braiding to wandering or to single-thread.

As for the causes, almost all the authors agree that the morphological changes are mainly to ascribe to human intervention especially at reach scale (embankments, groynes, levees, weirs, dams) and, after the 1950s, to the mining activity that caused an increasing rate of narrowing and incision.

After the Little Ice Age, climate changes seem to have played a minimal role as the analysis of the hydrological and climatic data does not reveal variations that could justify the observed morphological changes.

In our analysis of Taro River most of the narrowing (and the connected channel centerline shifting) result from the anthropic subtraction of wide riverbed portions for agricultural use, or from the reduction of the channel section for the construction of bridges and the relative bank protections. The mining strengthening after the 1950s seems to have caused mainly a strong incision while the consistent measured narrowing until 1990 is again to ascribe to the human removal of large portions of the river margins for facilities construction and for restoring of previous mining area. Rather debated are the changes in recent decades. Most of the studies claim a sure progressive channel widening, usually accompanied by aggrading, and attribute the trend inversion to the end of mining activity, dated around the middle of the 1980s. However in the Panaro River (Castaldini and Ghinoi, 2008) this trend inversion is not registered and the narrowing seems to continue nowadays. In Surian et al. (2009) a narrowing is described for the Torre River and in Ziliani and Surian (2012) the short term analysis of Tagliamento River from 1990 to 2009, reveals a moderate widening even if the rate of widening, as revealed by the four subperiods analysed, was highly variable and a slight channel narrowing occurred between 2001 and 2007. For Rinaldi et al. (2005) the recent widening and aggradation trend is registered along some reaches of the Vara R. and only locally along the Trebbia R. For Pellegrini et al. (2008) the width increasing in the two Alpine rivers analyzed seems associated to an extreme flood in 2000 after which a modest narrowing process restarted. For the Taro Rivers it seems evident from the short term analysis from 1999 to 2011 that the increase in widening is mainly due to the temporary effects of two great floods and a clear trend in widening cannot be established. Furthermore, in the lower single thread part of the channel the narrowing seems to continue.

6. Conclusions

The quantitative analysis of the planform changes in the Taro River has allowed to outline the channel evolution in the last 200 years.

The use of shell scripts based on the GRASS GIS commands made possible a fast calculation of the main morphological parameters and the drawing of graphics showing in great detail the continuous parameter variation along the entire channel development making unnecessary a prior channel segmentation. The analysis revealed a continuous channel width reduction, with variable speed, a braiding reduction, and a sinuosity increase, at least until the end of the 20th century, in agreement with most of the previous work carried out by other authors in other rivers both in Italy and abroad.

Less obvious is the most recent evolutionary trend that, contrary to what has been shown in other studies, would seem to be characterized by a substantial morphological stability in the upper part of the channel but by a slight persistent narrowing in the lower single-thread.

These variations can be substantially attributed to the human activity. In particular, the continuous narrowing is largely due to the recurrent subtraction of river areas to be assigned to agriculture and industry, and to the construction of as many as 10 bridges, with their up- and down-streams bank protections. Mining seems to have provoked a sharp incision and only partially a narrowing. The sporadic and discontinuous hydrological data show no substantial changes, and in agreement with the previous Authors, the contribution of changes in flow regime to the morphological changes can be considered negligible.

References

Ashmore, P., 1991. Channel morphology and the bed load pulses in braided, gravel-bed streams. *Geografiska Annaler*, 73A, 37-52.

Bernini, M., Papani, G., 1987. Alcune considerazioni sulla struttura del margine appenninico emiliano fra lo Stirone e l'Enza (e sue relazioni con il sistema del F. Taro). *Acta Naturalia de l'Ateneo Parmense*, 23 (4), 219-239.

Bertoldi, W., Zanoni, L., Tubino, M., 2010. Assessment of morphological changes induced by flow and flood pulses in a gravel bed braided river: The Tagliamento River (Italy). *Geomorphology* 114, 348-360.

Bizzarri, A., Terzi, F., 1984. L'evento meteo-alluvionale del novembre 1982 e i conseguenti dissesti nelle valli del Taro e del Ceno: cause e proposte operative. In: *Atti del Convegno sul dissesto territoriale del novembre 1982 nelle valli del Taro e del Ceno*, 13-31.

Castaldini D., Ghinoi, A., 2008. Recent morphological changes of the River Panaro (Northern Italy). *Il Quaternario, Italian Journal of Quaternary Sciences* 21, 267-278.

Cati L., 1984. L'evento alluvionale dell'8 e 9 novembre 1982 sul bacino del F. Taro. In: *Atti del Convegno sul dissesto territoriale del novembre 1982 nelle valli del Taro e del Ceno*, 35-61.

- Comiti, F., Da Canal, M., Surian, N., Mao, L., Picco, L., Lenzi, M.A., 2011. Channel adjustments and vegetation cover dynamics in a large gravel bed river over the last 200 years. *Geomorphology* 125, 147-159.
- Downward, S.R., Gurnell, A.M., Brookes, A., 1994. A methodology for quantifying river channel planform change using GIS. *Variability in stream erosion and sediment transport: Proceedings of the Canberra Symposium*. IAHS Publ. 224, 449-456.
- Egozi, R., Ashmore, P., 2008. Defining and measuring braiding intensity. *Earth Surf. Process. Landforms* 33, 2121-2138.
- Fisher, G.B., Bookhagen, B., Amos, C.B., 2013. Channel planform geometry and slopes from freely available high-spatial resolution imagery and DEM fusion: Implications for channel width scalings, erosion proxies, and fluvial signatures in tectonically active landscapes. *Geomorphology* 194, 46–56.
- FGDC, 1998. *Geospatial Positioning Accuracy Standards, Part 3: National Standard for Spatial Data Accuracy*. Standard Document: FGDC-STD-007-3-1998. Federal Geographic Data Committee: Reston, Virginia.
- GRASS Development Team, 2014. GRASS: geographic resources analysis support system, <http://grass.osgeo.org>.
- Gurnell, A.M., Downward, S.R., Jones, R., 1994. Channel planform change on the River Dee meanders, 1876–1992. *Regulated Rivers: Research & Management* 9, 187–204.
- Gurnell, A., Surian, N., Zanoni, L., 2009. Multi-thread river channels: A perspective on changing European alpine river systems. *Aquat. Sci.* 71, 253–265.
- Haiyong, L., Lihong, S., 2009. Double-line river axis extraction based on Delaunay triangulation. In: Yaolin L. and Xinming T. (Eds.), *Proc. SPIE 7492, International Symposium on Spatial Analysis, Spatial-Temporal Data Modeling, and Data Mining*, (October 13, 2009), 6 pp. <http://dx.doi.org/10.1117/12.838073>.
- Hughes, M. L., McDowell, P. F., Marcus, W. A., 2006. Accuracy assessment of georectified aerial photographs: Implications for measuring lateral channel movement in a GIS. *Geomorphology* 74, 1-16.
- Lauer, J.W., 2006. *Channel Planform Statistics Toolbox*. National Center for Earth-surface Dynamics. Minneapolis, MN 55414, http://www.nced.umn.edu/system/files/PlanformStatisticsTools_0.ppt.
- Leys, K.F., Werritty, A., 1999. River channel planform change: software for historical analysis. *Geomorphology* 29, 107–120.

- Lombardini, E., 1865. Della condizione idraulica della pianura subapennina fra l'Enza ed il Panaro. *Giornale dell'ingegnere, architetto ed agronomo* 13, 193-240.
- Mount, N.J., Louis, J., Teeuw, R.M., Zukowskyj, P.M., Stott, T., 2003. Estimation of error in bankfull width comparisons from temporally sequenced raw and corrected aerial photographs. *Geomorphology* 56, 65-77.
- Mount, N.J., Louis, J., 2005. Estimation and propagation of error in measurements of river channel movement from aerial imagery. *Earth Surf. Process. Landforms* 30, 635– 643.
- Neteler, M., Mitasova, H., 2008. *Open Source GIS: A GRASS GIS Approach*, third ed. Springer, 406 pp.
- Pavelsky, T.M., Smith, L.C., 2008. RivWidth: a Software Tool for the Calculation of River Widths From Remotely Sensed Imagery. *IEEE Geoscience and remote sensing letters*, 5 (1), 70-73.
- Pellegrini, L., Maraga, F., Turitto, O., Audisio, C., Duci, G., 2008. Evoluzione morfologica di alvei fluviali mobili nel settore occidentale del bacino padano. *Il Quaternario, Italian Journal of Quaternary Sciences* 21 (1B), 251-266.
- Pellegrini, M., Perego, S., Tagliavini, S., 1979. La situazione morfologica degli alvei degli affluenti emiliani del Po. In: *Atti del Convegno di idraulica padana*, 1-9.
- Perego, S., 1994. Evoluzione naturale e antropica del medio e basso corso del F.Taro (prov. di Parma). *Acta Naturalia de l'Ateneo Parmense* 30 (1/4), 5-27.
- Piégay, H., Alber, A., Slater, L., Bourdin, L., 2009. Census and typology of braided rivers in the French Alps. *Aquat. Sci.* 71, 371–388.
- Rinaldi, M., 2003. Recent channel adjustments in alluvial rivers of Tuscany, Central Italy. *Earth Surf. Process. Landforms* 28, 587–608.
- Rinaldi, M., Simoncini, C., Sogni, D., 2005. Variazioni morfologiche recenti di due alvei ghiaiosi appenninici: il fiume Trebbia ed il fiume Vara. *Geogr. Fis. Dinam. Quat. Suppl.* VII, 313-319.
- Segura-Beltrán, F., Sanchis-Ibor, C., 2013. Assessment of channel changes in a Mediterranean ephemeral stream since the early twentieth century. The Rambla de Cervera, eastern Spain. *Geomorphology* 201, 199-214.
- Schumm, S.A., 1963. Sinuosity of Alluvial Rivers on the Great Plains. *Geol. Soc. Am. Bull.* 74, 1089-1100.
- Surian, N., Rinaldi, M., 2003. Morphological response to river engineering and management in alluvial channels in Italy. *Geomorphology* 50, 307-326.

Surian, N., Ziliani, L., Cibien, L., Cisotto, A., Baruffi, F., 2008. Variazioni morfologiche degli alvei dei principali corsi d'acqua veneto-friulani negli ultimi 200 anni. *Il Quaternario, Italian Journal of Quaternary Sciences* 21 (1b), 279-290.

Tagliavini, S., 1975. Aspetti e problemi geomorfologici connessi con l'attività estrattiva dell'Emilia occidentale. In: *Atti del Convegno Cave e assetto del territorio*, 75-97.

Thorne, C.R., 1997. Channel types and morphological classification. In: Thorne, C.R., Hey, R.D., Newson, M.D. (Eds.), *Applied Fluvial Geomorphology for River Engineering and Management*. John Wiley & Sons Ltd., pp. 175-222.

Veggiani, A., 1984. Il deterioramento climatico dei secoli XVI-XVIII e i suoi effetti sulla bassa Romagna. *Studi romagnoli* 35, 109-124.

Ziliani, L., Surian, N., 2012. Evolutionary trajectory of channel morphology and controlling factors in a large gravel-bed river. *Geomorphology* 173-174, 104-117.

Appendice A (supplementary material)

Fig. 1-S. 1976 channel width graphic

Caption of Fig. 1-S.

Fig. 2-S. 1976 channel braiding graphic

Caption of Fig. 2-S.

Fig. 3-S. 1976 channel sinuosity graphic

Caption of Fig. 3-S.

Fig. 4-S. 1828-2011 channel shifting graphic

Caption of Fig. 4-S.

Fig. 5-S. Graphic of the channel width for all the nine considered dates.

Caption of Fig. 5-S.

Supp_09. 1976-1999 channel braiding graphic

Supp_10. Caption of Supp_09

Supp_11. 1976-1999 channel sinuosity graphic

Supp_12. Caption of Supp_11

Supp_14. Caption of Supp_13

Supp_16. Caption of Supp_15

Supp_17. 1828-1881-1958-1976-1999-2011 channel braiding graphic

Supp_18. Caption of Supp_17

Supp_19. 1828-1881-1958-1976-1999-2011 channel sinuosity graphic

Supp_20. Caption of Supp_19

Supp_21. 1828-1881-1958-1976-1999-2011 channel shifting graphic

Supp_22. Caption of Supp_21

Didascalie nel materiale supplementare.

Curve singole annate.

Channel width for the year 1976. In the lower x-axis the progressive distances from the origin are reported. On the upper x-axis the positions of the 57 reference points (R01-R57) projected on the channel centerline are reported together with their partial and cumulative distances. The channel width value is on the y-axis. All values are in meters. In addition to the curve of the original width values, the moving average curve of 21 terms is traced (thicker line). The horizontal and vertical scale are 1:50000 and 1: XXX respectively.

Braiding index for the year 1976. In the lower x-axis the progressive distances from the origin are reported. On the upper x-axis the positions of the 57 reference points (R01-R57) projected on the channel centerline are reported together with their partial and cumulative distances. All values are in meters. The braiding index is on the y-axis. In addition to the curve of the original braiding values, the moving average curve of 21 terms is traced (thicker line). The horizontal scale is 1:50000.

Sinuosity for the year 1976. In the lower x-axis the progressive distances from the origin are reported. On the upper x-axis the positions of the 57 reference points (R01-R57) projected on the channel centerline are reported together with their partial and cumulative distances. All values are in meters. The sinuosity value is on the y-axis. The horizontal scale is 1:50000.

Curve coppie annate.

Channel width for the years 1976 and 1999. In the lower x-axis the progressive distances from the origin are reported. On the upper x-axis the positions of the 57 reference points (R01-R57) projected on each channel centerline are reported together with their partial and cumulative distances. Because the channel length changes from date to date, the projections of the reference points change their positions along x –axis. The difference in distance between each couple of reference points from one date to the previous one, is a measure of the channel length change and is reported along the upper x-axis.

The channel width value is on the y-axis. All values are in meters. In addition to the curves of the original values, the moving average curves of 21 terms are also traced (thicker lines). The horizontal and vertical scale are 1:50000 and 1: XXX respectively.

Braiding index for the years 1976 and 1999. In the lower x-axis the progressive distances from the origin are reported. On the upper x-axis the positions of the 57 reference points (R01-R57) projected on each channel centreline are reported together with their partial and cumulative distances. Because the channel length changes from date to date, the projections of the reference points change their positions along x –axis. The difference in distance between each couple of reference points from one date to the previous one, is a measure of the channel length change and is reported along the upper x-axis. All values are in meters.

The braiding index is on the y-axis. In addition to the curves of the original braiding values, the moving average curves of 21 terms are traced (thicker lines). The horizontal scale is 1:50000.

Sinuosity for the years 1976 and 1999. In the lower x-axis the progressive distances from the origin are reported. On the upper x-axis the positions of the 57 reference points (R01-R57) projected on each channel centreline are reported together with their partial and cumulative distances. Because the channel length changes from date to date, the projections of the reference points change their positions along x –axis. The difference in distance between each couple of reference points from one date to the previous one, is a measure of the channel length change and is reported along the upper x-axis. All values are in meters.

The sinuosity value is on the y-axis. The horizontal scale is 1:50000.

Centerline shifting for the interval 1976-1999. In the lower x-axis the progressive distances from the origin are reported. On the upper x-axis the positions of the 57 reference points (R01-R57) projected on the centrelines axis are reported together with their partial and cumulative distances. The channel shifting value is on the y-axis. All values are in meters. In addition to the curves of the original shifting values, the moving average curve of 21 terms is traced (thicker line). The horizontal and vertical scale are 1:50000 and 1: respectively.

Curve multiple.

Channel width for years from 1828 to 2011. The short-term dates and intervals between 1999 and 2011, have been omitted due to the slight planimetric variations leading to an almost complete overlap of the curves. In the lower x-axis the progressive distances from the origin are reported. On the upper x-axis the positions of the 57 reference points (R01-R57) projected on each channel centerline are reported together with their partial and cumulative distances. Because the channel length changes from date to date, the projections of the reference points change their positions along

x –axis. The difference in distance between each couple of reference points from one date to the previous one, is a measure of the channel length change and is reported along the upper x-axis. The channel width value is on the y-axis. All values are in meters. In addition to the curves of the original width values, the moving average curves of 21 terms are traced (thicker lines). The horizontal and vertical scale are 1:50000 and 1: respectively.

Braiding index for years from 1828 to 2011. **The short-term dates and intervals between 1999 and 2011, have been omitted due to the slight planimetric variations leading to an almost complete overlap of the curves.** In the lower x-axis the progressive distances from the origin are reported. On the upper x-axis the positions of the 57 reference points (R01-R57) projected on each channel centreline are reported together with their partial and cumulative distances. Because the channel length changes from date to date, the projections of the reference points change their positions along x –axis. The difference in distance between each couple of reference points from one date to the previous one, is a measure of the channel length change and is reported along the upper x-axis. All values are in meters.

The braiding index is on the y-axis. In addition to the curves of the original braiding values, the moving average curves of 21 terms are traced (thicker lines). The horizontal scale is 1:50000.

Sinuosity for years from 1828 to 2011. **The short-term dates and intervals between 1999 and 2011, have been omitted due to the slight planimetric variations leading to an almost complete overlap of the curves.** In the lower x-axis the progressive distances from the origin are reported. On the upper x-axis the positions of the 57 reference points (R01-R57) projected on each channel centreline are reported together with their partial and cumulative distances. Because the channel length changes from date to date, the projections of the reference points change their positions along x –axis. The difference in distance between each couple of reference points from one date to the previous one, is a measure of the channel length change and is reported along the upper x-axis. All values are in meters.

The sinuosity value is on the y-axis. The horizontal scale is 1:50000.

Centerline shifting for the time intervals from 1828 to 2011. **The short-term dates and intervals between 1999 and 2011, have been omitted due to the slight planimetric variations leading to an almost complete overlap of the curves.** In the lower x-axis the progressive distances from the origin are reported. On the upper x-axis the positions of the 57 reference points (R01-R57) projected on the centrelines axis are reported together with their partial and cumulative distances. Because the centrelines axis length changes from one time interval to another, the projections of the reference points change their positions along x –axis. The difference in distance between each couple of reference points from one time interval to the previous one, is a measure of the axis length change and is reported along the upper x-axis. The channel shifting value is on the y-axis. All values are in meters. In addition to the curves of the original shifting values, the moving average curves of 21 terms are traced (thicker lines). The horizontal and vertical scale are 1:50000 and 1: respectively.

1. Introduction

2. The study reach

3. Methodology

3.1. Data sources

3.2. Error assessment

3.3. Computed parameters

4. Parameters calculation and graphics construction

5. Analysis of the results

5.1 Channel changes

5.1.1 Pre 1828

5.1.2 1828-1881

5.1.3 1881-1958

5.1.4 1958-1976

5.1.5 1976-1999

5.1.6 1999-2011

5.1.7 1828-2011

5.2 Comparison with previous works

6. Conclusions

References

Castaldini Dorianò - Full Professor - Department of Chemical and Geological Sciences, University of Modena and Reggio Emilia, Italy. doriano.castaldini@unimore.it

Pellegrini Luisa – Associated Professor - Department of Earth Sciences and Environment, University of Pavia, Italy. lpellegr@unipv.it

Rinaldi Massimo – Associated Professor - Department of Civil and Environmental Engineering, University of Firenze, Italy. mrinaldi@dicea.unifi.it

Segura-Beltrán Francesca - Full professor - Department of Geography, University of Valencia, Spain. Francisca.Segura@uv.es

Surian Nicola – Researcher – Department of Geosciences, University of Padova, Italy. nicola.surian@unipd.it

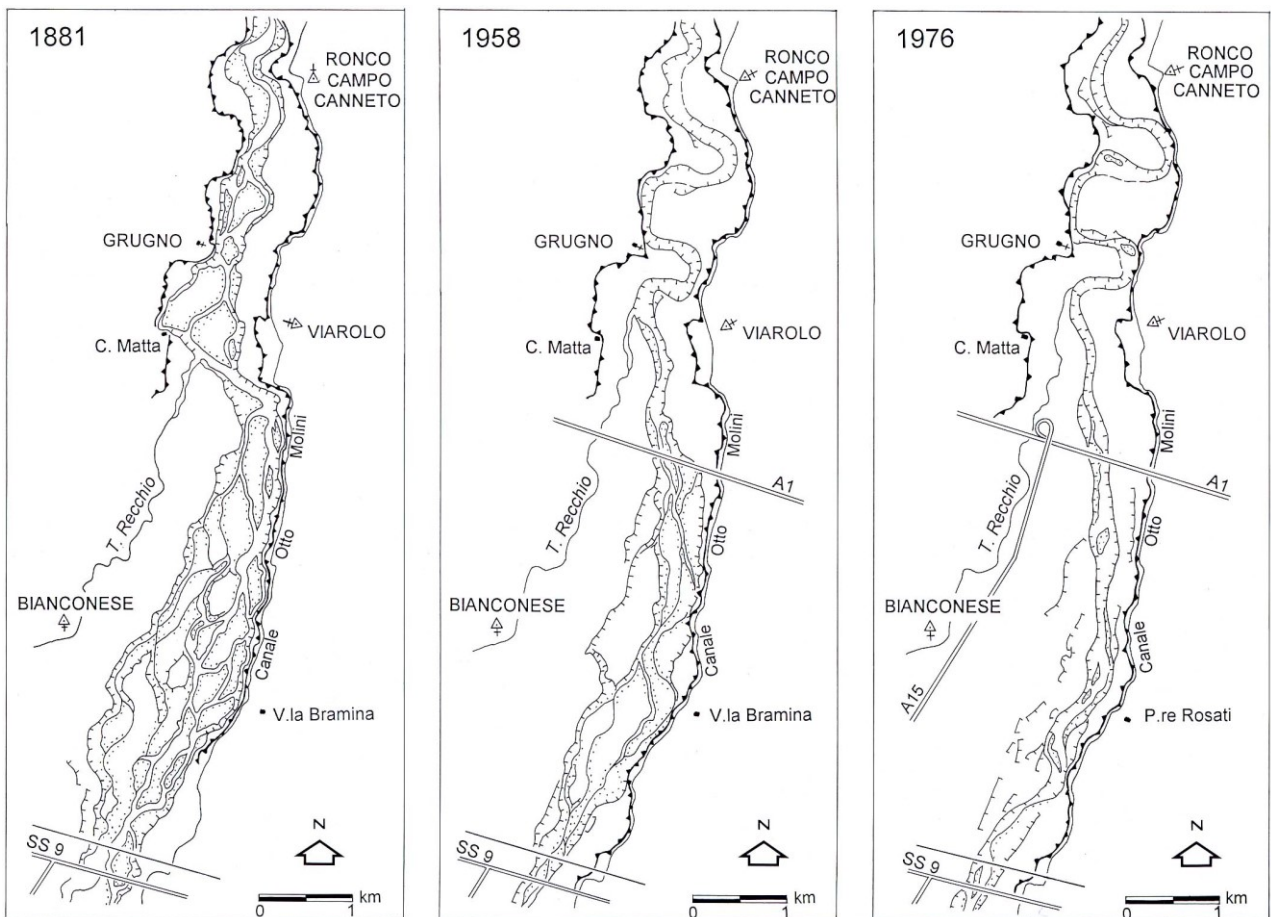


Fig. 7.4 Raffronto cartografico del tratto d'alveo a valle della via Emilia (SS9), in epoche diverse. La linea marcata con i triangolini indica l'argine maestro del F. Taro, la linea più sottile con i trattini gli orli di scarpata di terrazzo fluviale (da Perego, 1994).

Rinaldi, M., 2003. [Recent channel adjustments in alluvial rivers of Tuscany, central Italy. Earth Surface Processes and Landforms 28 \(6\), 587–608.](#)

Rinaldi, M., Wyzga, B., Surian, N., 2005. [Sediment mining in alluvial channels: physical effects and management perspectives. River Research and Applications 21 \(7\), 805–828.](#)

Rinaldi, M., Simoncini, C., Piégay, H., 2009. [Scientific design strategy for promoting sustainable sediment management: the case of the Magra River \(central-northern Italy\). River Research and Applications 25 \(5\), 607–625.](#)

Gurnell, A., Surian, N., Zanoni, L., 2009. [Multi-thread river channels: a perspective on](#)

changing European alpine river systems. *Aquatic Sciences—Research Across Boundaries* 71 (3), 253–265

Surian, N., Cisotto, A., 2007. Channel adjustments, bedload transport and sediment sources in a gravel-bed river, Brenta River, Italy. *Earth Surface Processes and Landforms* 32 (11), 1641–1656.

Surian, N., Rinaldi, M., 2003. Morphological response to river engineering and management in alluvial channels in Italy. *Geomorphology* 50 (4), 307–326.

Surian, N., Ziliani, L., Comiti, F., Lenzi, M.A., Mao, L., 2009. Channel adjustments and alteration of sediment fluxes in gravel-bed rivers of north-eastern Italy: potentials and limitations for channel recovery. *River Research and Applications* 25 (5), 551–567.

Zanoni, L., Gurnell, A., Drake, N., Surian, N., 2008. Island dynamics in a braided river from analysis of historical maps and air photographs. *River Research and Applications* 24 (8), 1141–1159.

Bertoldi, W., Zanoni, L., Tubino, M., 2009. Planform dynamics of braided streams. *Earth Surface Processes and Landforms* 34, 547–557

Pellegrini, L., Maraga, F., Turitto, O., Audisio, C., Duci, G., 2008. Evoluzione morfologica di alvei fluviali mobili nel settore occidentale del bacino padano. *Il Quaternario* 21 (1B), 251–266.

Surian, N., Mao, L., Giacomini, M., Ziliani, L., 2009c. Morphological effects of different channel-forming discharges in a gravel-bed river. *Earth Surface Processes and Landforms* 34 (8), 1093–1107.

Surian, N., Rinaldi, M., Pellegrini, L., Audisio, C., Maraga, F., Teruggi, L., Turitto, O., Ziliani, L., 2009d. Channel adjustments in northern and central Italy over the last 200 years. In: James, L.A., Rathburn, S.L., Whittecar, G.R. (Eds.), *Management and Restoration of Fluvial Systems with Broad Historical Changes and Human Impacts*. Special Paper, 451. Geological Society of America, Boulder, U.S.A., pp. 83–95.

Surian, N., Rinaldi, M., Pellegrini, L., 2011. Channel adjustments and implications for river management and restoration. *Geografia Fisica E Dinamica Quaternaria* 34 (1), 145

A marked phase of braiding expansion commencing in the Middle Ages, has also been recognized in the Alps and particularly in several French rivers (Bravard, 1989; Piegay et al., 2006), and was associated with catchment-wide pressures induced by an increasing rural population. Widespread deforestation occurred as agriculture expanded onto more marginal, often steeply-sloping, land, and overgrazing (*impoverire un pascolo*) was common on this cleared land as a result of relatively high stocking densities. These catchment-scale human activities increased runoff and sediment supply to river channels, leading to an increase in the magnitude and frequency of floods and the quantities of sediment that they transported, although Bravard (1989) has also attributed increases in sediment supply and braiding expansion to changes in climate, particularly during the Little Ice Age.

From the end of the 19th century and throughout the 20th century, human activities dramatically altered river dynamics so that the extent of braided and transitional river reaches were significantly reduced throughout Europe (Table 2). For example, during the 20th century, the total length of braided reaches decreased by 70% and 95%, respectively, in France and Austria (Habersack and Piegay, 2008; Muhar et al., 2008). Table 2 reports some cases of channel pattern change, for example from braiding to wandering or to single-thread, but there were also many sites where more subtle changes occurred, for example where braiding persisted but braiding intensity decreased significantly (see below). These morphological changes were caused by a range of human activities that affected both drainage basins and river channels, such as channelization, dam construction, flow regulation, sediment mining, land-use changes and torrent-control works. Complex sets of these activities altered flow regimes and particularly sediment fluxes, as well as channel boundary conditions. In particular, a decrease in bed-load supply to river channels has been identified as the driving factor of many channel adjustments (e.g. Kondolf et al., 2002; Surian et al., 2009). The case studies reported in Table 2 illustrate that in some rivers a cumulative effect of many different human activities has occurred, whereas in others one or two activities are thought to be responsible for channel changes. Furthermore, there are cases where basin-scale activities are identified as the major cause of channel change (e.g. land-use change, afforestation, torrent-control works; see Begueria et al., 2006; Kondolf et al., 2007), whereas in other cases reach scale interventions were more significant (e.g. sediment mining; see Wishart et al., 2008; Surian et al., 2009).

In order to delve more deeply into the causes and consequences of the transformation of European river channel styles, we now focus on some Italian examples. Here, multi-thread and transitional rivers are very common both in rivers draining from the Alps and from the Apennines. These Italian rivers have experienced widespread channel adjustments over the last 200 years, in particular incision, narrowing and changes in channel pattern (e.g. Castiglioni and Pellegrini, 1981; Castaldini and Piacente, 1995; Surian and Rinaldi, 2003; Rinaldi, 2003; Surian and Rinaldi, 2004; Surian, 2006; Surian and Cisotto, 2007). Surian et al. (2009), in a recent study of 12 of these braided and transitional rivers, identified the following

Cronache sulla legislazione in materia (Pellegrini)

Channel outlines were digitized directly from the photographs. One operator carried out all of the digitizing for the purposes of consistency. Channel banks could be easily detected, although in some areas of dense riparian tree cover the bank position had to be interpolated between areas where the bank was visible (generally 10 m in length). Field validation of the interpolation demonstrated that this caused errors of no more than 1 m. Control points composed of four or more field boundaries and building corner locations were also recorded from each photograph in order to rectify the vector file to a base map (1975 UK Ordnance Survey 1:10000 map) using a least squares solution. Once the channel outline had been constructed for each date, the planform maps were overlain to form an accurate picture of channel change for the study reach between 1988 and 1994 (e.g. Figure 2). (Winterbottom and Gilvear, 2000)

6.3.1. Temporal variability of width adjustments

Changes in the channel width are related to the contrasted effects caused by large and minor events in ephemeral streams. **Large floods exceed the critical shear stress for erosion, transport larger amounts of sediment through the system and produce channel changes whose effects may persist for many years.** Minor events do not always exhibit the shear stress required to mobilise the channel-bed material, and therefore, **could contribute to narrowing and stabilisation by vegetation** (Hooke and Mant, 2002). Thus, during the dry periods, vegetation can easily colonise bars and islands, boosting narrowing processes. This could be the main cause of the radical narrowing documented in the Rambla de Cervera between 1946 and 1956, similar to the Nahal Hoga case study (Rozin and Schick, 1996), attributed to a decrease of 9% in the runoff–rainfall ratio between 1940 and 1960. **On the other hand, large floods or intense sequences of large floods, such as the period 1962–1971 or the flood of 2000 in the Rambla de**

Cervera, slowed or stopped the narrowing trend, because of the erosional work carried out in some areas of the river bed.

These large events are responsible for the major channel changes, and in many occasions only mobilise material from the river bed (Hooke and Mant, 2002). **Francisca Segura-Beltrán a,* , Carles Sanchis-Ibor b 2013**

Both climate and human activities underwent important fluctuations since the beginning of the twentieth century, **although we cannot exactly determine the influence of each of these factors on the river's morphological evolution.** Some of these factors produce contradictory effects, affecting flow, sediment dynamics, and vegetation cover.

Short-term channel adjustments mainly depend on magnitude, frequency, and timing of the floods.

Long-term changes are influenced by sediment fluxes, flow and flood characteristics, and interaction of sediment and vegetation. In general terms, the alteration of sediment fluxes has been a major factor driving such channel adjustments, and it was mainly caused by land use changes and gravel mining. **Francisca Segura-Beltrán a,* , Carles Sanchis-Ibor**

b 2013

river segmentation

However, there is an additional problem associated with air photograph interpretation in that the **identification of the bank location is not as clear-cut as when using maps.**

Although historical analysis of braiding intensity can be affected by significant errors, notably the impact of river stage at the time of mapping / photography on estimates

but because of unknown mapping conventions, quantitative comparison with features identified from aerial photographs was uncertain

Sediment removal or 'mining', particularly during the 1970s and 1980s, has resulted in bed incision that is particularly marked between river kilometres 114 and 123. Incision has been accompanied by narrowing of the active corridor and a reduction in the braiding index. Whilst we have no quantitative information on the timing or severity of such mining activities in the Tagliamento's middle and upper reaches, it is likely that gravel mining has occurred, particularly during construction works for the A23 motorway and in association with building repairs and reconstruction following the 1976 earthquake.

. Maximum bankfull width change between images exceeds measurement error in all change periods. However, mean bankfull width change never exceeds the error. In such situations, it is important to quote maximum and mean changes